THE JOURNAL OF PHYSICAL CHEMISTRY A

Feature Article

pubs.acs.org/JPCA

Formation Mechanisms of Naphthalene and Indene: From the Interstellar Medium to Combustion Flames

Alexander M. Mebel,*[,†] Alexander Landera,[‡] and Ralf I. Kaiser*[,§]

[†]Department of Chemistry and Biochemistry, Florida International University, Miami, Florida 33199, United States

[‡]Chemical Sciences and Engineering Division, Argonne National Laboratory, Argonne, Illinois 60439, United States

[§]Department of Chemistry, University of Hawaii at Manoa, Honolulu, Hawaii 96822, United States

Supporting Information

ABSTRACT: The article addresses the formation mechanisms of naphthalene and indene, which represent prototype polycyclic aromatic hydrocarbons (PAH) carrying two six-membered and one five- plus a six-membered ring. Theoretical studies of the relevant chemical reactions are overviewed in terms of their potential energy surfaces, rate constants, and product branching ratios; these data are compared with experimental measurements in crossed molecular beams and the pyrolytic chemical reactor emulating the extreme conditions in the interstellar medium (ISM) and the combustion-like environment, respectively. The outcome of the reactions potentially producing naphthalene and indene is shown to critically depend on temperature and pressure or collision energy and hence the reaction mechanisms and their contributions to the PAH growth can be rather different in the ISM, planetary atmospheres, and in combustion flames at different temperatures and pressures. Specifically, this paradigm is illustrated with new theoretical results for rate constants and product branching ratios for the reaction of phenyl radical with vinylacetylene. The analysis of the formation mechanisms of naphthalene and its derivatives shows that in combustion they can be produced via hydrogen-abstraction-acetylene-addition (HACA) routes, recombination of cyclopentadienyl radical with itself and with cyclopentadiene, the reaction of benzyl radical with propargyl, methylation of indenyl radical, and the reactions of phenyl radical with vinylacetylene and 1,3-butadiene. In extreme astrochemical conditions, naphthalene and dihydronaphthalene can be formed in the C_6H_5 + vinylacetylene and C_6H_5 + 1,3-butadiene reactions, respectively. Ethynyl-substituted naphthalenes can be produced via the ethynyl addition mechanism beginning with benzene (in dehydrogenated forms) or with styrene. The formation mechanisms of indene in combustion include the reactions of the phenyl radical with C_3H_4 isomers allene and propyne, reaction of the benzyl radical with acetylene, and unimolecular decomposition of the 1-phenylallyl radical originating from 3-phenylpropene, a product of the C_6H_5 + propene reaction, or from C_6H_5 + C_3H_5.

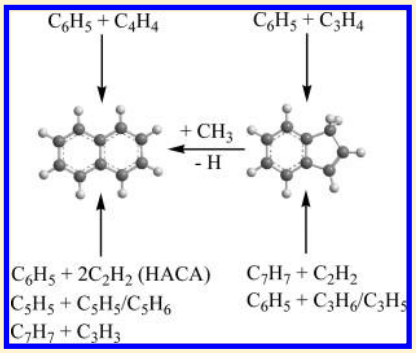

1. INTRODUCTION

Polycyclic aromatic hydrocarbons (PAH) and soot commonly formed as a result of incomplete combustion are major pollutants hazardous for human health and the ecosystem.[1] Though harmful to the life forms on Earth, in astrochemistry and astrobiology PAH are linked to the prebiotic evolution of the interstellar medium (ISM).[2−4] PAHs are present in circumstellar envelopes of carbon rich asymptotic giant branch (AGB) stars and account for up to 20% of the cosmic carbon budget. Such omnipresence of PAHs in interstellar space has been inferred from observations of the diffuse interstellar bands (DIBs)—discrete absorption features ranging from the blue part of the visible (400 nm) to the near-infrared (1200 nm) overlaid well with the interstellar extinction curve[5−8]—and from the unidentified infrared (UIR) emission bands probed in the range 3−14 μm.[7,9,10] PAHs have been identified in carbonaceous chondrites such as Murchison, where the measured $^{13}C/^{12}C$ isotopic ratios unambiguously confirmed that they were formed in the interstellar medium, most likely in the circumstellar envelope of carbon rich AGB stars.[11]

Achieving a detailed understanding of PAH and soot formation processes, from elementary chemical reactions initiating and propagating the growth of PAH at the molecular level to successive nucleation of soot particles, particle coagulation and their surface growth, is an important research goal in terms of both the basic science (evolution of prebiotic molecules in interstellar space) and engineering (minimizing the PAH yield in combustion and development of cleaner combustion processes and devices). The formation and growth mechanism of PAHs is enormously complex, with a large array of possible reactions arising from the great variety of molecules and radicals that are present in different isomeric forms.[12−15] The reactions involved occur over intricate potential energy surfaces with multiple local minima and products and hence their mechanisms, rates, and product yields may strongly depend on the conditions under which they take place.

Received: September 26, 2016
Revised: November 17, 2016
Published: January 10, 2017

ACS Publications © 2017 American Chemical Society

DOI: 10.1021/acs.jpca.6b09735
J. Phys. Chem. A 2017, 121, 901−926

Scheme 1

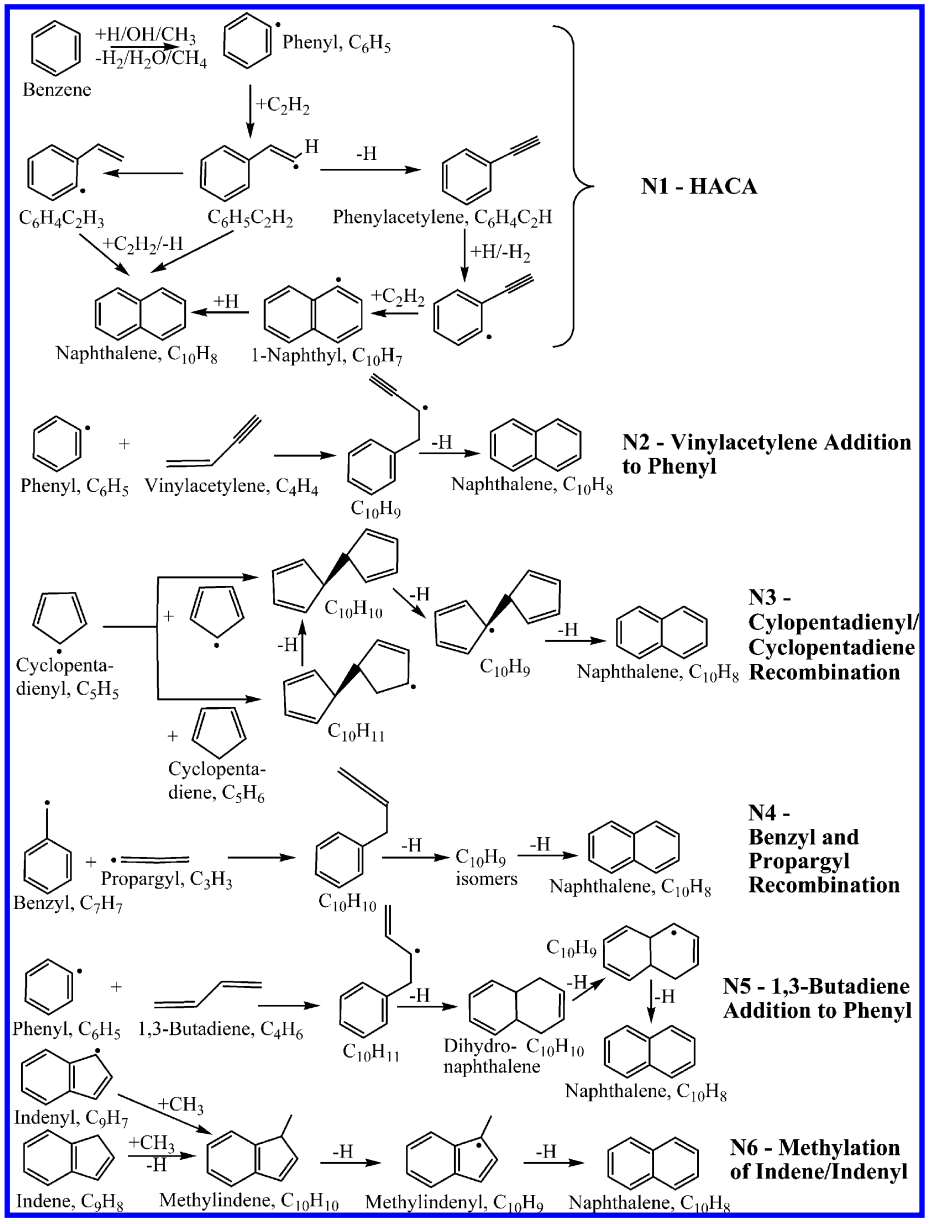

A principal task for general understanding the molecular evolution of PAH is unraveling the elementary step of PAH expansion by one extra ring, which could be an additional six-member or five-member ring. The prototype of this elementary step is the formation of naphthalene or indene from benzene, i.e., the step from one aromatic ring to two aromatic rings. To comprehend the mechanism and kinetics of this prototype growth step in this paper, we overview potential reaction mechanisms for the formation of naphthalene and indene from smaller molecules and radicals. We demonstrate that the outcome of the relevant chemical reactions critically depends on temperature and pressure or collision energy and hence the reaction mechanisms and their contributions to the PAH growth can be rather different in the ISM, planetary atmospheres, and in combustion flames at different temperatures and pressures. Specifically, we present new calculation results for rate constants and product branching ratios for the reaction of phenyl radicals (C_6H_5) with vinylacetylene (C_4H_4) illustrating this paradigm.

Whereas laboratory experiments can probe chemical reactions in terms of their kinetics, dynamics, and product distribution only at a limited set of conditions depending on a particular experimental technique, theoretical calculations are possible for a much broader range of the reaction conditions as long as the physical principles underlying the theory remain valid. In the meantime, theories used in the prediction of reaction mechanisms and product branching ratios are not exact and can achieve only limited accuracy depending on the computational efforts and available computing resources. Therefore, the validation of theoretical predictions vs available experimental results is absolutely essential to make them trustworthy and to evaluate their error bars. In this Article, we illustrate the synergism between theory and experiment in the studies of elementary chemical reactions producing the two smallest and prototypical PAH molecules, naphthalene and indene.

DOI: 10.1021/acs.jpca.6b09735
J. Phys. Chem. A 2017, 121, 901−926

Scheme 2

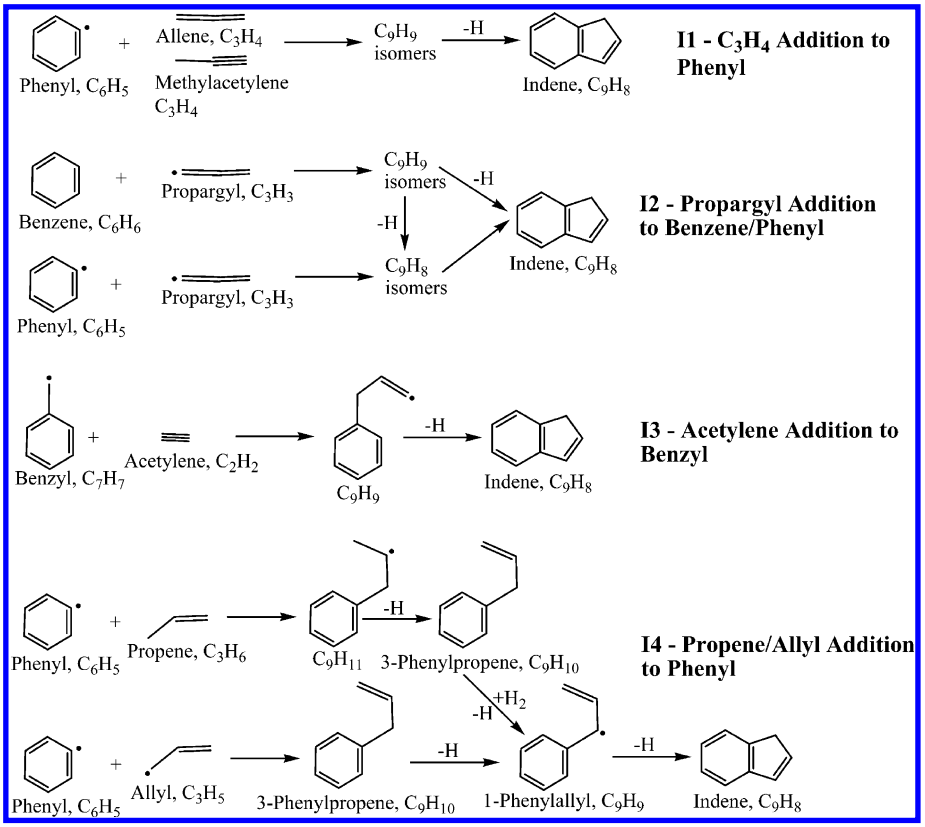

2. OVERVIEW OF FORMATION MECHANISMS OF NAPHTHALENE AND INDENE

Naphthalene consists of two fused aromatic six-member rings and has a $C_{10}H_8$ stoichiometry. The molecule can be synthesized from smaller species through chemical reactions involving $C_{10}H_x$ potential energy surfaces (PES), where x varies from 6 to 11. The reactions occurring on the $C_{10}H_x$ surfaces ($x \geq 9$) may form hydrogenated naphthalenes and then produce naphthalene after consecutive dehydrogenation steps. Alternatively, the reactions involving PES with $x = 6$ and 7 can lead to naphthalene via hydrogen atom additions if hydrogen atoms are available. One of the reactants usually contains an aromatic six-member ring so that the reaction can proceed as molecular growth from one ring to a two-ring aromatic structure. It is also possible that the reactants include five-member rings rather than a six-member ring. Several reactions or reaction sequences have been proposed and studied theoretically and experimentally as a potential source of naphthalene. They include (Scheme 1):

(N1) Hydrogen abstraction acetylene addition (HACA) sequences,

$$C_6H_6(\text{benzene}) + H/CH_3/OH \rightarrow C_6H_5(\text{phenyl radical}) + H_2/CH_4/H_2O$$

$$C_6H_5 + C_2H_2 \rightarrow C_8H_7(C_6H_5C_2H_2 \text{ or } C_6H_4C_2H_3) \rightarrow C_8H_6(C_6H_5C_2H, \text{phenylacetylene}) + H$$

$$C_8H_7 + C_2H_2 \rightarrow C_{10}H_9 \rightarrow C_{10}H_8(\text{naphthalene}) + H$$

$$C_6H_5C_2H + H \rightarrow C_6H_4C_2H + H_2$$

$$C_6H_4C_2H + C_2H_2 \rightarrow C_{10}H_7(\text{naphthyl radical})$$

$$C_{10}H_7 + H \rightarrow C_{10}H_8(\text{naphthalene})$$

(N2) Addition of vinylacetylene to phenyl radical,

$$C_6H_5 + C_4H_4 \rightarrow C_{10}H_9 \rightarrow C_{10}H_8 + H$$

(N3) Recombination of two cyclopentadienyl radicals and the reaction of cyclopentadienyl with cyclopentadiene,

$$C_5H_5 + C_5H_5 \rightarrow C_{10}H_{10} \rightarrow C_{10}H_9 + H$$

$$C_{10}H_9 \rightarrow C_{10}H_8 + H$$

$$C_5H_5 + C_5H_6 \rightarrow C_{10}H_{11} \rightarrow C_{10}H_{10} + H \rightarrow \ldots \rightarrow C_{10}H_8 + 3H$$

(N4) Reactions of propargyl radical with benzyl radical,

$$C_7H_7(\text{benzyl}) + C_3H_3 \rightarrow C_{10}H_{10} \rightarrow C_{10}H_9 + H \rightarrow C_{10}H_8 + 2H$$

DOI: 10.1021/acs.jpca.6b09735
J. Phys. Chem. A 2017, 121, 901−926

(N5) Addition of 1,3-butadiene to phenyl radical,

$$C_6H_5 + C_4H_6(1,3\text{-butadiene}) \rightarrow C_{10}H_{11} \rightarrow C_{10}H_{10}(\text{dihydronaphthalene}) + H$$

$$C_{10}H_{10} \rightarrow C_{10}H_9 + H \rightarrow C_{10}H_8 + 2H$$

(N6) Conversion of indene or indenyl radical to naphthalene via methylation,

$$C_9H_8(\text{indene}) + CH_3 \rightarrow C_{10}H_{11} \rightarrow C_{10}H_{10}(\text{methylindene}) + H$$

$$C_{10}H_{10}(\text{methylindene}) \rightarrow C_{10}H_9(\text{methylindenyl}) + H$$

$$C_9H_7(\text{indenyl}) + CH_3 \rightarrow C_{10}H_{10}(\text{methylindene}) \rightarrow C_{10}H_9(\text{methylindenyl}) + H$$

$$C_{10}H_9(\text{methylindenyl}) \rightarrow C_{10}H_8 + H$$

Indene is the smallest PAH molecule, which contains one six- and one five-member ring with the C_9H_8 molecular formula. Reactions producing indene generally involve C_9H_x PESs (x = 8−11) and in particular, the following systems need to be considered (Scheme 2):

(I1) Reactions of phenyl radical with allene and propyne,

$$C_6H_5(\text{phenyl}) + C_3H_4(\text{allene or propyne}) \rightarrow C_9H_9 \rightarrow C_9H_8 + H$$

(I2) Reactions of propargyl radical with benzene and phenyl radical,

$$C_6H_6(\text{benzene}) + C_3H_3(\text{propargyl}) \rightarrow C_9H_9 \rightarrow C_9H_8 + H$$

$$C_6H_5 + C_3H_3 \rightarrow C_9H_8$$

(I3) A reaction of benzyl radical with acetylene,

$$C_7H_7(\text{benzyl}) + C_2H_2 \rightarrow C_9H_9 \rightarrow C_9H_8 + H$$

(I4) Reactions of phenyl radical with propene and allyl radical,

$$C_6H_5 + C_3H_6(\text{propene}) \rightarrow C_9H_{11} \rightarrow C_9H_{10}(\text{3-phenylpropene}) + H$$

$$C_9H_{10}(\text{3-phenylpropene}) + H \rightarrow C_9H_9(\text{1-phenylallyl}) + H_2$$

$$C_9H_9(\text{1-phenylallyl}) \rightarrow C_9H_8 + H$$

$$C_6H_5 + C_3H_5(\text{allyl}) \rightarrow C_9H_{10} \rightarrow C_9H_9(\text{1-phenylallyl}) + H \rightarrow C_9H_8 + 2H$$

In this Article, we briefly review experimental and theoretical data on these reaction mechanisms reported by our and other groups and focus on the $C_6H_5 + C_4H_4$ reaction, which helps us illustrate a strong dependence of the reaction outcome on the conditions, such as temperature (or bimolecular collision energy) and pressure. We begin with a short description of the experimental and theoretical methods that are employed by our groups to unravel reaction mechanisms for naphthalene and indene formation and to predict or identify the reaction products.

3. EXPERIMENTAL SECTION

3.1. Crossed Molecular Beam Setup. The crossed molecular beam technique represents an unprecedented approach to reveal the outcome of a reaction of two neutral molecules, radicals, and/or atoms in the single collision environment *without* wall effects.[16−19] This is achieved by generating supersonic beams of the reactants in separate side chambers and crossing them in the main reaction chamber. For example, the supersonic phenyl-radical beam is generated by flash pyrolysis of helium-seeded nitrosobenzene at seeding fractions of typically less than 0.1%.[20] A chopper wheel located after the pyrolysis section and behind the skimmer selects a well-defined velocity of the pulsed radical beam, which in turn results in a precise collision energy between the primary and secondary beams. The secondary reactants, the hydrocarbons, are introduced via the secondary source chamber. The reaction products are detected by a rotatable triply differentially pumped mass spectroscopic detector within the plane of the primary and secondary beams. The neutral products are *universally* electron impact ionized at 80 eV before being mass selected at a specific mass-to-charge ratio (m/z) and detected under ultrahigh vacuum conditions as low as 10^{-11} Torr. The reactive scattering signal at a well-defined mass-to-charge ratio is recorded at multiple angles exploiting the time-of-flight (TOF) technique by recording the flight time versus the ion counts of an ion of the selected mass-to-charge ratio (m/z); the collision between the radical and the hydrocarbon molecule defines the "time zero" in each experiment. At each angle, the TOFs are integrated, providing a laboratory angular distribution, which reports the integrated ion counts at a defined mass-to-charge ratio versus the laboratory angle. These laboratory data (laboratory angular distribution, TOF spectra) are then transformed into the center-of-mass reference frame exploiting a forward deconvolution technique.[21,22] This yields two crucial functions, which allow us to extract the reaction dynamics and underlying reaction mechanisms: the center-of-mass angular distribution ($T(\theta)$) and the product translational energy distribution ($P(E_T)$). The final result is the generation of a product flux contour map, $I(\theta,u) = P(u) \times T(\theta)$, which reports the flux of the reactively scattered products (I) as a function of the center-of-mass scattering angle (θ) and product velocity (u). This map can be seen as the *image of the chemical reaction* and contains *all* the information on the scattering process.

3.2. Pyrolytic Reactor. "High-temperature" experiments simulating combustion-like conditions or the outflow of carbon rich stars such as IRC+10216 are carried out at the Advanced Light Source (ALS) at the Chemical Dynamics Beamline (9.0.2.) utilizing a "pyrolytic reactor", which consists of a

DOI: 10.1021/acs.jpca.6b09735
J. Phys. Chem. A 2017, 121, 901−926

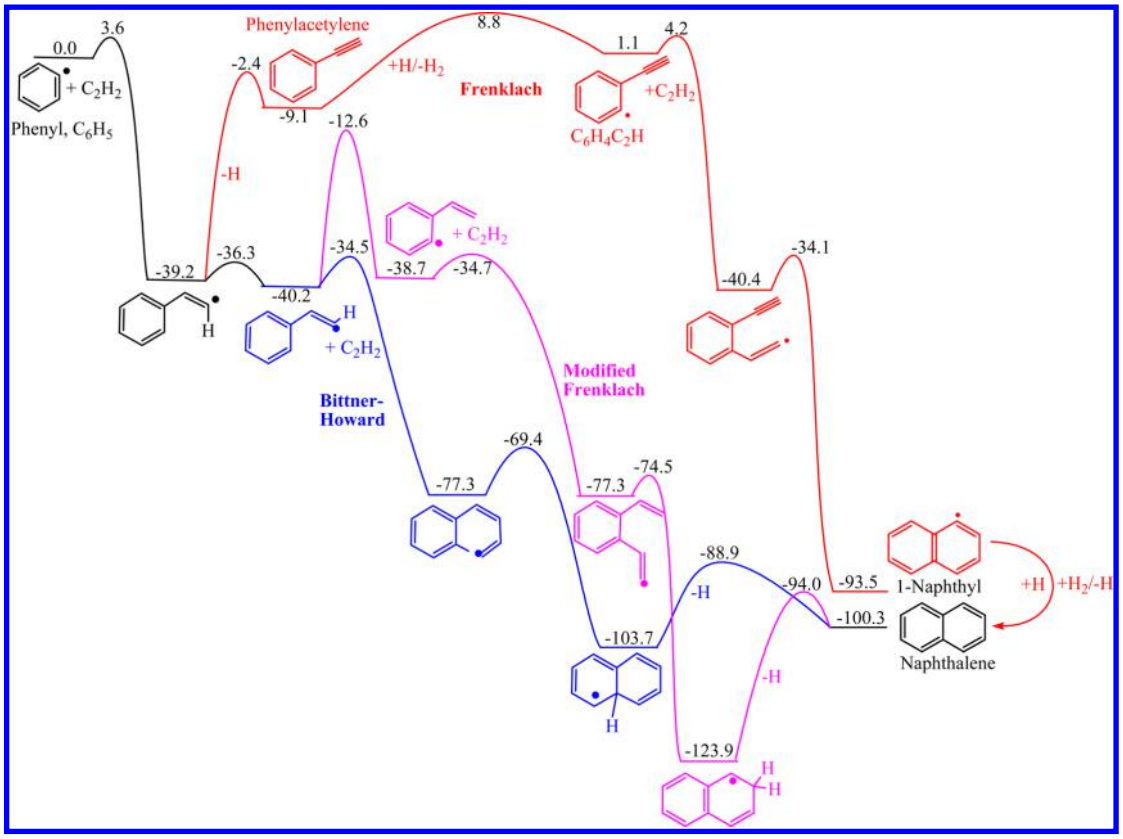

Figure 1. Potential energy diagram for various HACA routes. All relative energies are given in kcal/mol.

resistively heated silicon carbide nozzle operated at temperatures of typically 1000 K.[23] Phenyl radicals are generated at concentrations of less than 0.1% in situ via quantitative pyrolysis of nitrosobenzene (C_6H_5NO) seeded in a carrier gas (for instance, acetylene, C_2H_2, or allene or propyne, C_3H_4), which also serves as a second reactant. After exiting the pyrolytic reactor, the molecular beam passes a skimmer and enters a detection chamber containing a Wiley−McLaren reflectron time-of-flight (ReTOF) mass spectrometer. The products are photoionized in the extraction region of the spectrometer by exploiting quasi continuous tunable vacuum ultraviolet (VUV) light from the Chemical Dynamics Beamline 9.0.2 of the Advanced Light Source and detected with a microchannel plate (MCP) detector. As the synchrotron light is quasi-continuous (500 MHz), a start pulse for the time-of-flight (TOF) ion packet is provided by pulsing the repeller plate (the lowest electrode in the Wiley−McLaren ion optics) of the time-of-flight ion optics. The ions hit the MCP detector; the signal from these ions are collected with a multichannel-scalar card (NCS; FAST Comtec 7886) triggered by the repeller plate pulse. Time-of flight spectra, which report the flight time of the ion versus the intensity of the ion counts, are recorded for the photoionization energy range between 8.0 and 10.0 eV. The photoionization efficiency (PIE) curves of a well-defined ion of a mass-to-charge ratio (m/z) can be obtained by plotting the integrated ion signal at the mass-to-charge versus the photoionization energy between 8.0 and 10.0 eV, normalized by the photon flux and the number of laser shots. The synchrotron VUV photon flux is measured by a calibrated silicon photodiode. Each PIE curve at a well-defined mass-to-charge ratio can then be fit by a linear combination of known PIE curves of all structural isomers.

4. THEORETICAL METHODS: AB INITIO/RRKM AND RRKM-ME CALCULATIONS OF REACTION RATE CONSTANTS AND PRODUCT BRANCHING RATIOS

PESs of chemical reactions described in this Article were computed at the G3(MP2,CC)//B3LYP/6-311G(d,p) level of theory,[24−26] which is capable of providing a chemical accuracy of 1−2 kcal/mol for the energetics. Most of the surfaces have been published in previous works[27−44] but here we included, using the same theoretical level, several additional, potentially important reaction channels that were not considered earlier. The ab initio calculations were performed using the GAUSSIAN 09[45] and MOLPRO 2010[46] program packages. The energies and molecular parameters of the reactants, reaction intermediates, transition states, and products were utilized in Rice−Ramsperger−Kassel−Marcus (RRKM) calculations of rate constants of elementary reaction steps. For single-collision conditions in crossed molecular beam experiments approaching the zero-pressure limit, we employed the microcanonical version of RRKM theory and computed collision energy-dependent rate constants and relative yields of potential products. Here, rate constant $k(E)$ at an internal energy E for a unimolecular reaction A* → A# → P is given by[47]

$$k(E) = \frac{\sigma}{h}\cdot\frac{W^{\#}(E - E^{\#})}{\rho(E)}$$

where σ is the reaction path degeneracy, h is the Plank constant, $W^{\#}(E-E^{\#})$ is the total number of states for the transition state A# with a barrier $E^{\#}$, and $\rho(E)$ is the density of states of the energized reactant molecule A*. The available internal energy E is taken as a sum of the reaction collision energy E_{col} and the

DOI: 10.1021/acs.jpca.6b09735
J. Phys. Chem. A 2017, 121, 901−926

energy of chemical activation, i.e., the negative of the relative energy of an intermediate or a transition state with respect to the separated reactants. With the RRKM computed rate constants, kinetic equations for unimolecular reactions are expressed as

$$\frac{d[C]_i}{dt} = \sum k_n[C]_j - \sum k_m[C]_i$$

where $[C]_i$ and $[C]_j$ are concentrations of various intermediates or products, and are solved within the steady state approximation. This approach[48] allows us to evaluate product branching ratios with the assumption that the reaction system behaves statistically and that the intramolecular vibrational redistribution (IVR) process is faster than any unimolecular reaction step. A drawback of this method is that it does not take into account radiative stabilization of reaction intermediates, which may be significant at very low temperatures relevant to astrochemical environments, as will be shown for the C_6H_5 + C_4H_4 system.

For thermal conditions at finite pressures, phenomenological rate constants are computed by solving the one-dimensional master equation[49] employing the MESS package.[50] Here, rate constants $k(T)$ for individual reaction steps are calculated within RRKM (unimolecular reactions) or transition state theory (TST, bimolecular reactions) generally utilizing the rigid-rotor, harmonic-oscillator (RRHO) model for the calculations of densities of states and partition functions for molecular complexes and the number of states for transition states. Soft normal modes are visually examined and those representing internal rotations are treated as one- or two-dimensional hindered rotors in partition function calculations. Respective one- and two-dimensional torsional potentials are calculated by scanning PESs at the B3LYP/6-311G(d,p) level of theory.

The computational strategies used to generate collision parameters required for solving the master equation and thus for taking into account pressure-dependent collision deactivation/activation of intermediates have been described in detail earlier.[51] Collisional energy transfer rates in the master equation are expressed using the "exponential down" model,[52] with the temperature dependence of the range parameter α for the deactivating wing of the energy transfer function expressed as $\alpha(T) = \alpha_{300}(T/300\ K)^n$, with $n = 0.62$ and $\alpha_{300} = 424\ cm^{-1}$ obtained earlier from classical trajectories calculations.[53] For the C_6H_5 + C_4H_4 system, we used the Lennard-Jones parameters (ε/cm^{-1}, σ/Å) = (390, 4.46) calculated earlier using the "one-dimensional optimization" method[54] for the similar naphthyl radical ($C_{10}H_7$) + Ar system.[28]

5. NAPHTHALENE FORMATION MECHANISMS

5.1. HACA Sequences (N1). The HACA mechanism was first proposed by Frenklach and co-workers.[55−60] For the production of naphthalene from benzene, HACA involves H abstraction forming the phenyl radical followed by addition of two acetylene molecules. After a first C_2H_2 molecule adds to phenyl producing a $C_6H_5C_2H_2$ radical, the addition of a second acetylene molecule can occur in three different ways (Figure 1): (i) to the ortho carbon in the ring after an H loss leading to phenylacetylene $C_6H_5C_2H$ and activation of the latter by intermolecular H abstraction in the ortho position (the ensuing six-member ring closure in $C_6H_4(C_2H)(C_2H_2)$ produces the naphthyl radical (the original Frenklach route)), (ii) to the side chain of $C_6H_5C_2H_2$ giving $C_6H_5CHCHCHCH$ followed by six-member ring closure and H loss producing naphthalene (the Bittner−Howard route),[61] and (iii) to the ortho C in the ring after intramolecular isomerization of $C_6H_5C_2H_2$ to $C_6H_4C_2H_3$ (the $C_6H_4(C_2H_3)(C_2H_2)$ radical produced after the C_2H_2 addition ring-closes and loses an extra hydrogen giving naphthalene (the modified Frenklach route)). More than two decades ago, Wang and Frenklach first computed PESs for various HACA reactions at a semiempirical AM1 level of theory and performed calculations of temperature- and pressure-dependent rate constants using RRKM theory.[57] Following their pioneering work, several high-level ab initio studies for critical HACA steps were reported;[27,62−64] however, except for the C_6H_5 + C_2H_2 reaction,[63] rate constant calculations were limited to the high-pressure (HP) limit. In our most recent work, we generated temperature- and pressure-dependent rate constants and product branching ratios for the HACA sequences from benzene to naphthalene utilizing more accurate G3(MP2,CC) PESs and the modern RRKM-ME approach for rate constant calculations.[28] This allowed us not only to update the HACA rate expressions for kinetic models of PAH formation in flames, most of which still use the old AM1/RRKM results from Wang and Frenklach[57] but also to make important qualitative conclusions on the potential relevance of various HACA routes under different combustion conditions.

We found that the C_8H_7 radicals, $C_6H_5C_2H_2$ and $C_6H_4C_2H_3$, are unstable at high temperatures and low pressures because they cannot be collisionally stabilized at the atmospheric pressure and below at temperatures of 1650 K and higher. This makes both the Bittner−Howard and the modified Frenklach HACA routes unrealistic under typical low-pressure flame conditions. At higher pressures the C_8H_7 radicals may contribute significantly to the formation of naphthalene because naphthalene has been shown to be the predominant product of the $C_6H_5C_2H_2$ + C_2H_2 and $C_6H_4C_2H_3$ + C_2H_2 reactions in the entire 500−2500 K range independent of pressure. In the meantime, the equilibrium between C_6H_5 + C_2H_2 and C_8H_7 is reversed at high temperatures, which will hinder these routes greatly. The original Frenklach HACA route is shown to preferentially form a dehydrogenated naphthalene core (naphthyl radicals or naphthynes) for $T < 2000$ K and to produce mostly a non-PAH diethynylbenzene product at higher temperatures. The results of our calculations indicate that the role of HACA in the formation of naphthalene from benzene may be overstated by the current kinetic models, but more quantitative conclusions on the role of HACA in the formation of a second aromatic ring should await the inclusion of the new temperature- and pressure-dependent rate coefficients for the HACA reactions as well as for other possible naphthalene formation pathways in flame modeling studies.

Our recent experimental work[65] confirmed, for the first time, that the reaction of phenyl with two acetylene molecules indeed forms naphthalene. Naphthalene and the HACA byproduct phenylacetylene $C_6H_5C_2H$ were synthesized in the pyrolitic chemical reactor at a temperature of 1020 ± 100 K. The interpretation of the measured mass spectrum gave clear evidence of the production of hydrocarbons with the molecular formulas C_8H_6 and $C_{10}H_8$. The identification of the product isomers was based on an analysis of the PIE curves as a function of photon energy. The experimental PIE curves matched closely to the reference photoionization efficiency curves of phenylacetylene (C_8H_6) and naphthalene ($C_{10}H_8$) isomers. We

DOI: 10.1021/acs.jpca.6b09735
J. Phys. Chem. A 2017, 121, 901−926

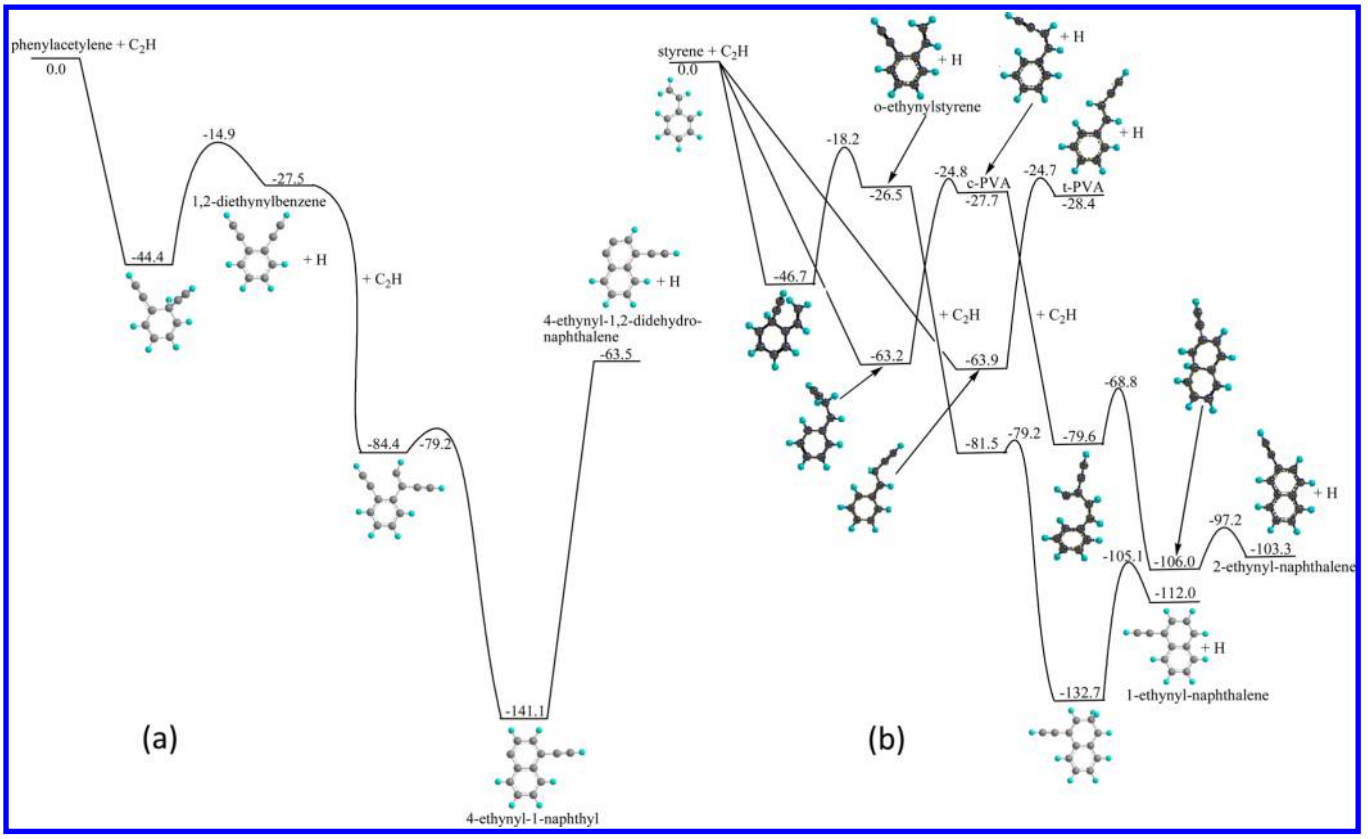

Figure 2. Potential energy diagrams for the ethynyl addition mechanism for the formation of a naphthalene core initiating from phenylacetylene (a) and styrene (b). All relative energies are given in kcal/mol.

were able to conclude that phenylacetylene and naphthalene are solely responsible for the products at m/z 102 and 128 and determined their relative yields as 95 ± 1% and 5 ± 1%, respectively. The detection of naphthalene together with phenylacetylene successfully demonstrated reaction pathways corresponding to HACA sequences. However, the original Frenklach route that involves the formation of phenylacetylene, followed by hydrogen abstraction from the phenyl ring leading to a $C_6H_4C_2H$ radical, was ruled out because no evidence for a second hydrogen abstraction from phenylacetylene was observed. If a second hydrogen atom abstraction occurred, products from acetylene addition to the meta and para positions of the aromatic ring, which do not cyclize to naphthyl radical but rather form 1,3- and 1,4-diethynylbenzenes $C_{10}H_6$ by H elimination, would have been observed but no products with the (m/z = 126) mass-to-charge ratio were detected. Apparently, under the experimental conditions in the chemical reactor at 1020 K the original Frenklach route was not efficient and the formation of naphthalene can be rationalized by the reaction mechanism proceeding through a second acetylene addition to C_8H_7 radicals, by either the modified Frenklach or Bittner−Howard routes.

The subsequent experimental study[66] in the chemical reactor corroborated the hypothesis that the $C_6H_5C_2H_2$ + C_2H_2 and $C_6H_4C_2H_3$ + C_2H_2 reactions form naphthalene. In fact, the naphthalene molecule was produced via a directed synthesis of the styrenyl $C_6H_5C_2H_2$ and of the *o*-vinylphenyl $C_6H_4C_2H_3$ transients with acetylene in the high-temperature (1500 ± 50 K) chemical reaction separately. The styrenyl and the *o*-vinylphenyl radicals were generated via pyrolysis of *β*-bromostyrene and 2-bromostyrene (C_8H_7Br), respectively. These precursors were seeded in neat acetylene at 400 Torr, which in turn was expanded into the chemical reactor. According to the mass spectra, the $C_{10}H_8$ product was synthesized via the reactions of the C_8H_7 radicals with a single acetylene molecule accompanied by the emission of one hydrogen atom. The experimental PIE curve of the $C_{10}H_8$ product was reproduced exceptionally well with the reference PIE curve of naphthalene for both the styrenyl in acetylene and *o*-vinylphenyl in acetylene systems and we concluded that naphthalene represents the sole contributor to signal at m/z = 128. Interestingly, in these systems a $C_{10}H_6$ product (m/z = 126) was also detected and might originate from diethynylbenzene isomers or from didehydronaphthalene, of which the only available reference PIE curve of 1,4-diethynylbenzene was overlaid well with the experimental curve. This indicates that the original Frenklach HACA sequence is more efficient at 1500 K than at 1020 K in the previous experiment. Here, the C_8H_7 radicals first dissociated to phenylacetylene, which was then activated by H abstraction and the C_8H_5 + C_2H_2 reactions formed the $C_{10}H_6$ products after hydrogen atom elimination.

5.2. Ethynyl Addition Mechanism. The experimental studies and theoretical calculations described above showed that the HACA mechanism can contribute to the formation of naphthalene from benzene under particular combustion conditions, such as at relatively low combustion temperatures (below 1650 K) and the atmospheric or lower pressure or at higher temperatures but at pressures above 10 atm. However, because of the existence of significant barriers both for the H abstraction and for acetylene addition steps, HACA is unlikely to be a significant source of naphthalene in harsh astrochemical conditions, i.e., at very low temperatures prevailing in planetary

DOI: 10.1021/acs.jpca.6b09735
J. Phys. Chem. A 2017, 121, 901−926

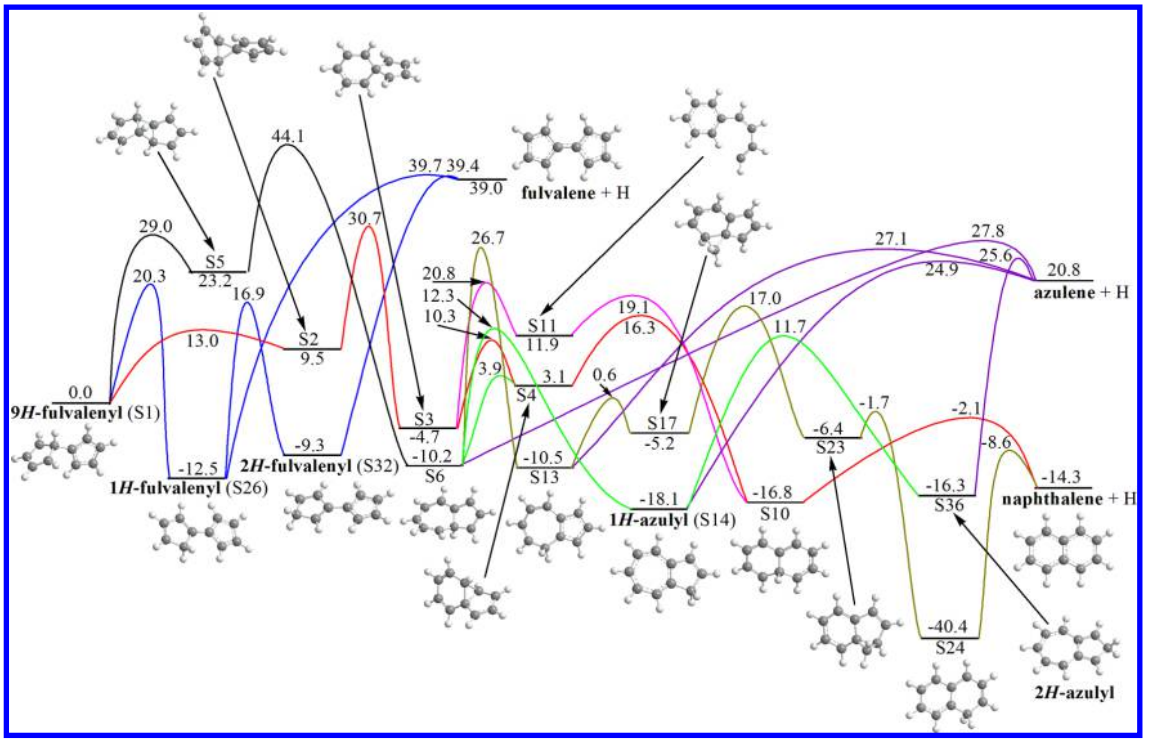

Figure 3. Potential energy diagram of isomerization and dissociation pathways of *n*H-fulvalenyl and *n*H-azulyl radicals. All energies are given in kcal/mol. Fulvalene and azulene formation pathways are shown in blue and purple, respectively. The spiran pathway to naphthalene is shown in red and the β-scission subpath is shown in magenta. Pathways from *n*H-azulyl radicals merging onto the spiran pathway are shown in green. The methylene walk pathway is shown in dark yellow.

atmospheres, such as that of Titan, or in cold molecular clouds. As an alternative to HACA for such conditions, we proposed a photoinduced ethynyl addition mechanism (EAM), which can produce C_2H-substituted naphthalene or a naphthalene core as in didehydronaphthalene or in naphthyl radical.[67] For instance, the rate constant for acetylene addition to phenyl between 100 and 200 K typical for the PAH-forming region in Titan's atmosphere is evaluated to be very low, in the 8.4×10^{-23} to 1.6×10^{-17} cm^3 molecule^{-1} s^{-1} range.[63] On the contrary, phenylacetylene can be formed via an alternative reaction, $C_6H_6 + C_2H \rightarrow C_6H_5C_2H + H$, which proceeds by barrierless addition of the ethynyl radical (C_2H) to benzene followed by a hydrogen atom elimination in an overall exoergic process.[68,69] This pathway has been found to be very fast at low temperatures, with $k = (3.0–4.0) \times 10^{-10}$ cm^3 molecule^{-1} s^{-1} at 105−298 K,[70] and the reaction product was confirmed as phenylacetylene by crossed molecular beams experiments.[71] Our ab initio calculations[67] of the PES have shown that after a barrierless addition of the ethynyl radical to the ortho carbon atom in phenylacetylene, the adduct is expected to rapidly lose a hydrogen atom, forming 1,2-diethynylbenzene (Figure 2a). 1,2-Diethynylbenzene can then react with a second ethynyl radical via addition to a carbon atom of one of the ethynyl side chains without entrance barriers, and the ensuing ring closure in the complex leads to an ethynyl-substituted naphthyl radical. Under single collision conditions as present in the interstellar medium, the radical loses a hydrogen atom to form ethynyl-substituted 1,2-didehydronaphthalene; this process can compete only with radiative stabilization of the radical. On the contrary, under higher pressures as present, for example, in Titan's atmosphere, the C_2H-substituted naphthyl radical can be stabilized by collisions. For the analogous C_2H + styrene ($C_6H_5C_2H_3$) reaction (Figure 2b),[72] which also proceeds without a barrier, the dominant routes are H atom eliminations from the initial adducts; C_2H addition to the vinyl side chain of styrene is predicted to produce trans- or cis-conformations of phenylvinylacetylene (t- and c-PVA), whereas C_2H addition to the ortho carbon in the ring is expected to lead to the formation of *o*-ethynylstyrene. Next, *cis*-phenylvinylacetylene and *o*-ethynylstyrene may undergo a second barrierless C_2H addition to ultimately produce ethynyl-substituted naphthalene derivatives, such as 1-ethynylnaphthalene in the case of ethynyl addition to the side chain in *o*-ethynylstyrene and 2-ethynylnaphthalene for C_2H additions to c-PVA. Because the C_2H + styrene → t-PVA + H/c-PVA + H/*o*-ethynylstyrene, C_2H + c-PVA → 2-ethynylnaphthalene + H, and C_2H + *o*-ethynylstyrene → 1-ethynylnaphthalene + H reactions are predicted to have no entrance barriers and to be highly exoergic, with all intermediates, transition states, and products lying much lower in energy than the initial reactants, they are anticipated to be fast even at very low temperature conditions prevailing in Titan's atmosphere or in the interstellar medium. In the regions where styrene and C_2H are available and overlap, the sequence of two C_2H additions can result in the closure of a second aromatic ring and thus provide a viable low-temperature route to the formation of 1- or 2-ethynylnaphthalene. The extrapolation of this mechanism provides a general growth step from a vinyl-substituted PAH to an ethynyl-substituted PAH with an extra aromatic ring. We anticipate the EAM to be of great importance to form PAH-like structures in the interstellar medium and in hydrocarbon-rich, low temperature atmospheres of planets and their moons such as Titan, where ethynyl radicals are readily available through a photolysis of abundant acetylene by photons with $\lambda < 217$ nm. Experimental verification of the EAM beyond the formation of pheynylacetylene by C_2H addition to benzene still awaits.

DOI: 10.1021/acs.jpca.6b09735
J. Phys. Chem. A 2017, 121, 901−926

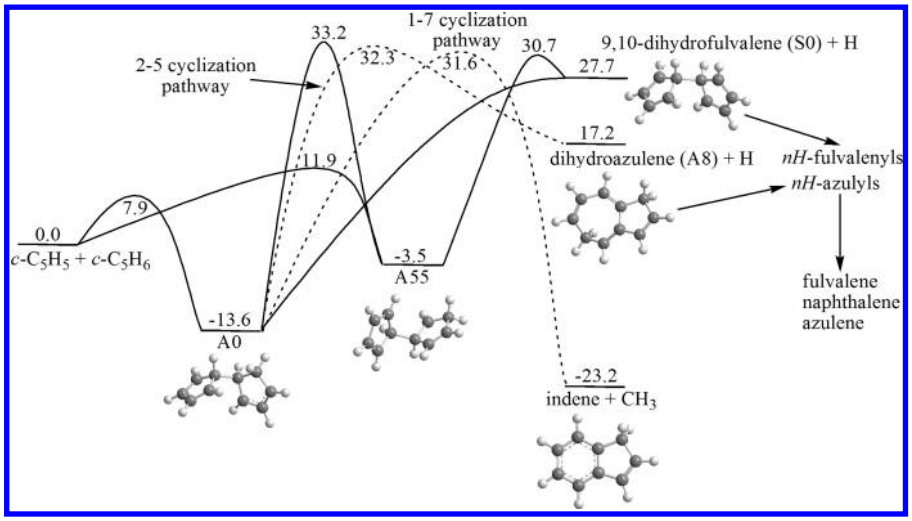

Figure 4. Potential energy diagram for the reaction of cyclopentadienyl radical with cyclopentadiene. All energies are given in kcal/mol. Dashed lines schematically show multistep pathways with the number indicating the highest in energy TS along the path. Details for these pathways are provided in ref 31.

5.3. C_5H_5 + C_5H_5/C_5H_6 Reactions (N3). Dean[73] was the first to suggest that recombination of two cyclopentadienyl radicals, *c*-C_5H_5, can form naphthalene together with molecular hydrogen. Melius et al.[74] later calculated the $C_{10}H_{10}$ PES and concluded that the more likely reaction channel is H elimination from the initial adduct producing the 9*H*-fulvalenyl radical. This conclusion was verified by higher level ab initio calculations of the $C_{10}H_{10}$ surface by our group, which confirmed that the pathway to naphthalene involving the H_2 loss is not competitive.[30] Melius et al. proposed that 9*H*-fulvalenyl eventually decomposes to naphthalene + H via a so-called spiran mechanism. Following their study, kinetic modelers began to include the *c*-C_5H_5 + *c*-C_5H_5 → naphthalene + 2H reaction in the PAH formation mechanisms and tried to fit the reaction rate expression based on experimental data from flame studies.[13,14,75−79] Cavallotti and Polino[80] have recently reported first-principles-based rate constant calculations for the *c*-C_5H_5 + *c*-C_5H_5 reactions in which they utilized a CBS-QB3 computed PES in conjunction with the RRKM-ME approach. This work gave a number of interesting conclusions. First, instead of immediately losing a hydrogen atom and forming 9*H*-fulvalenyl, the initial *c*-C_5H_5−*c*-C_5H_5 adduct (9,10-dihydrofulvalene) is more likely to undergo one or more H migrations and then to dissociate to 1*H*-fulvalenyl or 2*H*-fulvalenyl, which are calculated to be 9−12 kcal/mol more favorable than 9*H*-fulvalenyl. Moreover, isomerizations on the $C_{10}H_{10}$ PES can result in opening of one of the five-member ring and a ring reclosure can then produce a seven-member ring fused with the remaining five-member ring. H eliminations from such bicyclic $C_{10}H_{10}$ intermediates form 1*H*-azulyl and 2*H*-azulyl radicals, 16−18 kcal/mol more stable than 9*H*-fulvalenyl. Rate constant calculations at 1 bar showed that the *n*H-azulyl formation channels prevail in the temperature range of 1100−1500 K, whereas in the 1500−2000 K interval the formation of the *n*H-fulvalenyl radicals is more favorable. The rate constants for the cyclopenadienyl recombination reaction producing the $C_{10}H_9$ radicals were computed to be rather high, in the range of 10^{-13}−10^{-12} cm^3 $molecule^{-1}$ s^{-1}. Hence, if the *n*H-fulvalenyl and *n*H-azulyl radicals can efficiently decompose to naphthalene + H, the *c*-C_5H_5 + *c*-C_5H_5 reaction can indeed contribute into the formation of naphthalene in combustion.

Since the work by Melius and co-workers,[74] the pathways from *n*H-fulvalenyl radicals to naphthalene as well as H-assisted azulene-to-naphthalene isomerization were investigated by Alder et al.[81] and Wang et al.[82] In 2007, our group reported the most detailed G3(MP2,CC) study of the pertinent region of the $C_{10}H_9$ PES combined with rate constant calculations of individual reaction steps at the high-pressure limit.[29] Figure 3 shows the calculated potential energy diagram for the most favorable naphthalene formation pathways from *n*H-fulvalenyls and *n*H-azulenyls, which are predicted to be the primary products of *c*-C_5H_5 + *c*-C_5H_5. 1- and 2*H*-fulvalenyl radicals can directly dissociate to fulvalene + H overcoming barriers of 52.2 and 48.7 kcal/mol, respectively. On the contrary, 9*H*-fulvalenyl does not lose an H atom directly but has to first isomerize to 1*H*-fulvalenyl or further to 2*H*-fulvalenyl. The most favorable pathway from *n*H-fulvalenyl radicals to naphthalene in terms of enthalpy is the spiran route proposed by Melius et al.,[74] (2*H*-fulvalenyl, S32 → 1*H*-fulvalenyl, S26 →) 9*H*-fulvalenyl, S1 → S2 → S3 → S4 → S10 → naphthalene + H, with the highest in energy transition state (TS) corresponding to the S2 → S3 step (a hydrogen shift between two spiran-like intermediates) and residing 43.2, 40.0, and 30.7 kcal/mol above 1-, 2-, and 9*H*-fulvalenyls, respectively. An alternative within the spiran pathway, S3 → S11 → S10, called a *β*-scission mechanism, apparently is less competitive than S3 → S4 → S10 because of significantly higher barriers. Though the naphthalene product channel from *n*H-fulvalenyls is favored by enthalpy, the direct H losses to form fulvalene are preferable by the entropy factor. Therefore, the pathways to naphthalene and fulvalene are expected to compete, with the latter gaining significance at higher temperatures. Reaction channels leading from 1- and 2*H*-azulyl radicals to naphthalene merge with the spiran pathway at S4 via the following sequence, (2*H*-azulyl, S36 →) 1*H*-azulyl, S14 → S6 → S4, and the critical TS on the path from them to naphthalene corresponds to the S4 → S10 step and resides 34.4 and 32.6 above 1- and 2*H*-azulyls, respectively. Direct H elimination from 1- and 2*H*-azulyls radicals producing azulene exhibits higher barriers, 43.0 and 41.9 kcal/mol, respectively, but may become important at higher temperatures due to lower entropy demands. The methylene walk pathway, S6 → S13 → S17 → S23 → S24 → naphthalene + H, is

DOI: 10.1021/acs.jpca.6b09735
J. Phys. Chem. A 2017, 121, 901−926

unlikely to contribute to naphthalene formation from *nH*-fulvalenyls owing to very high barriers on the S1 → S5 → S6 path but may play a minor role in the conversion of *nH*-azulyl where S6 can be accessed directly from S14. Still, the barrier for S6 → S13 is 22.8 kcal/mol higher than for S6 → S4 and hence the spiran channel should be preferable.

Detailed calculations of the temperature- and pressure-dependent rate constants using the RRKM-ME approach for the *c*-C_5H_5 + *c*-C_5H_5 reaction, for unimolecular thermal decomposition of its primary products, *nH*-fulvalenyls and *nH*-azulyls, and for related secondary reactions, such as H-assisted isomerization of fulvalene and azulene to naphthalene, is on our future agenda. In the meantime, a qualitative conclusion can be made on the basis of the PES that the recombination of two cyclopentadienyl radicals is likely to represent an important source of naphthalene in combustion. The *nH*-fulvalenyl and *nH*-azulyl radicals are likely unstable at high temperatures due to relatively low dissociation barriers and even if they do not decompose to naphthalene, fulvalene or azulene may be efficiently converted to naphthalene via secondary reactions with hydrogen atoms. On the contrary, in interstellar environments or in reducing planetary atmospheres at low temperatures, the formation of naphthalene from *c*-C_5H_5 + *c*-C_5H_5 is not likely. The primary reaction products, the *nH*-fulvalenyl and *nH*-azulyl radicals, are endoergic and they need to overcome 30−50 kcal/mol barriers to split another H atom. Hence, the pathways to naphthalene can be realized only at high temperatures.

The reaction of cyclopentadienyl radical with cyclopentadiene was also considered as a potential source of two-ring PAHs, naphthalene and indene, at high temperatures.[31,78] The PES for the *c*-C_5H_5 + *c*-C_5H_6 reaction computed in the work by our group at the G3(MP2,CC) level of theory is extremely complex.[31] Nevertheless, as seen in Figure 4 summarizing the reaction channels most favorable energetically, we can expect that only few pathways can actually contribute. Cyclopentadienyl can add to cyclopentadiene in ortho or meta position with respect to the CH_2 group overcoming significant entrance barriers of 7.9 and 11.9 kcal/mol and forming $C_{10}H_{11}$ adducts A0 and A55, respectively. Both of the adducts can dissociate by losing a hydrogen atom to the 9,10-dihydrofulvalene $C_{10}H_{10}$ product either without an exit barrier (A0) or with a small exit barrier of 3.0 kcal/mol (A55). The *c*-C_5H_5 + *c*-C_5H_6 → 9,10-dihydrofulvalene + H reaction is 27.7 kcal/mol endoergic. Alternatively, A0 can be converted to a dihydroazulene isomer A8 + H or to indene + CH_3 via multistep pathways involving 1−7 or 2−5 cyclization of the initial complex A0. The critical barriers along these pathways are 31.6 and 32.3 kcal/mol relative to the initial reactants, respectively, i.e., slightly higher than the barriers required for the immediate H losses from A0 and A55. However, the complex multistep pathways to dihydroazulene and indene are much more entropically demanding and hence we anticipate 9,10-dihydrofulvalene to be the dominant if not exclusive reaction product at combustion temperatures. This hypothesis needs to be verified by future RRKM-ME calculations of the reaction rate constants and product branching ratios. The anticipated main reaction product, 9,10-dihydrofulvalene, is the initial adduct for the *c*-C_5H_5 + *c*-C_5H_5 reaction considered above and, according to the results by Cavallotti and Polino,[80] this adduct can undergo unimolecular decomposition to *nH*-fulvalenyl and *nH*-azulyl radicals, which in turn can dissociate to fulvalene, naphthalene, or azulene by splitting one more hydrogen atom. Dihydroazulene can also decompose to *nH*-azulyls. Thus, the *c*-C_5H_5 + *c*-C_5H_6 reaction can be a source of naphthalene and indene in combustion flames but its actual contribution depending on conditions is yet to be determined through calculations of the rate constants and inclusion them into kinetic flame models. However, due to the high reaction barriers and endoergicity, the reaction of cyclopentadienyl radical with cyclopentadiene is not important at low temperatures of the ISM and in planetary atmospheres.

5.4. C_7H_7 + C_3H_3 Reaction (N4). Colket and Seery[83] and later Marinov et al.[84] proposed that the reaction of benzyl and propargyl radicals, C_7H_7 + C_3H_3 → naphthalene + H + H, can contribute to the formation of naphthalene in flames. This reaction has been included in several kinetic models[85−87] and the first physics-based detailed calculations of the reaction mechanism and rate constants were reported by Matsugi and Miyoshi.[88] Using the density functional B3LYP and ab initio CBS-QB3 and CASPT2 methods, they mapped out the reaction PES, the pertinent region of the $C_{10}H_{10}$ surface, and utilized it in RRKM-ME calculations of rate constants at various temperatures and pressures. Matsugi and Miyoshi found that the dominant reaction channel is the addition of the propargyl radical to the CH_2 group of benzyl and then isomerization reaction pathways of the initial adduct followed by H elimination mostly produce the 1-methylene-2-indanyl radical at temperatures above 1500 K and also a certain amount of 1-methylene-3-indanyl. Subsequently, the 1-methyleneindanyl radicals are predicted to rapidly lose one more hydrogen atom and dissociate to either 1-methyleneindene or naphthalene + H. As a result of their study, Matsugi and Miyoshi put forward the following simplified mechanism for the conversion of benzyl + propargyl to naphthalene:

$$C_7H_7 + C_3H_3 \rightarrow \text{1-methylene-2-indanyl/1-methylene-3-indanyl} + H$$

$$\text{1-methylene-2-indanyl/1-methylene-3-indanyl} \rightarrow \text{1-methyleneindene} + H$$

$$\text{1-methylene-2-indanyl/1-methylene-3-indanyl} \rightarrow \text{naphthalene} + H$$

$$\text{1-methyleneindene} + H \rightarrow \text{naphthalene} + H$$

and generated temperature- and pressure-dependent rate expressions for kinetic modeling.

In our recent work,[37] we revisited the same region of the $C_{10}H_9$ surface at the G3(MP2,CC) level in relation to the mechanism of conversion of indene to naphthalene via methylation and computed RRKM-ME rate constants for unimolecular decomposition of the 1-methyleneindanyl radicals and for H-assisted isomerization of 1-methyleneindene (benzofulvene) to naphthalene in the temperature range of 500−2500 K and at pressures of 30 Torr and 1, 10, and 100 atm. The results corroborate the conclusions by Matsugi and Miyoshi[88] and show that 1-methylene-2-indanyl is unstable with respect to dissociation to 1-methyleneindene and naphthalene at temperatures above 1250, 1500, 1650, and 2000 K at 30 Torr and 1, 10, and 100 atm, respectively, and its lifetime at 1500 K and 1 atm is 0.035 μs. At lower temperatures, this radical predominantly decomposes to 1-methyleneindene. 1-Methylene-3-indanyl is even less stable than 1-methylene-2-

DOI: 10.1021/acs.jpca.6b09735
J. Phys. Chem. A 2017, 121, 901−926

indanyl and lasts up to 1125, 1375, 1500, and 1800 K at 30 Torr, 1, 10, and 100 atm, respectively, with the computed lifetime at 1375 K and 1 atm being ~0.03 μs. Thus, both 1-methyleneindanyl $C_{10}H_9$ radicals produced in the benzyl + propargyl reaction are not likely to be stable under combustion flame conditions and would rapidly decompose to the $C_{10}H_8$ isomers 1-methyleneindene and naphthalene, with the former largely favored. We have also reported rate constants for the 1-methyleneindene + H reaction and its particular product channels. The reaction was shown to be very fast, with rate constants in the range 2.1×10^{-11} to 2.8×10^{-10} cm^3 molecule^{-1} s^{-1} at T = 500−2500 K (3.1×10^{-11} cm^3 molecule^{-1} s^{-1} at 1500 K and 1 atm). At lower temperatures, stabilization of the $C_{10}H_9$ intermediate 1-methylindenyl is preferable, but at higher temperatures naphthalene + H are the predominant reaction products. The switch between the stabilization and dissociation happens at 1375, 1650, 2000, and 2500 K for pressures of 30 Torr, 1, 10, and 100 atm, respectively.

The C_7H_7 + C_3H_3 reaction is an important source of naphthalene in combustion but, similarly to c-C_5H_5 + c-C_5H_5, is not expected to form naphthalene in low-temperature environments. Although the reaction is barrierless in the entrance channel, the prevailing 1-methyleneindanyl products are exoergic by only ~15 kcal/mol but they need at least 36 kcal/mol of internal energy to eliminate another H atom.

5.5. Reaction of Phenyl Radical with 1,3-butadiene (N5). The reaction of phenyl with 1,3-butadiene has been shown to form dihydronaphthalene both under single-collision (zero-pressure) conditions in crossed molecular beams[38] and under combustion-like conditions in the chemical reactor.[39] For instance, the crossed beam reactions of C_6H_5 with C_4H_6 and fully deuterated C_4D_6 as well as of the phenyl-d_5 radical C_6D_5 with 1,3-butadiene-2,3-d_2 and 1,3-butadiene-1,1,4,4-d_4 at collision energies of ~13 kcal/mol gave the bicyclic 1,4-dihydronaphthalene molecule as a major product of this reaction (58 ± 15%) with the 1-phenyl-1,3-butadiene being a relatively minor product (34 ± 10%). On the basis of the observed mass spectra, we identified the formation of $C_{10}H_{10}$ isomer(s) plus atomic hydrogen and the product isomer was assigned by considering the reaction energetics, i.e., by comparing the experimentally determined reaction energy of 28.7 ± 7.2 kcal/mol derived from the $P(E_T)$ distribution with the energies of various $C_{10}H_{10}$ isomers calculated theoretically. The experimental reaction exoergicity best matches the theoretically predicted value for the 1,4-dihydronaphthalene, 23.4 ± 2 kcal/mol within the error limits. The second closest exoergic product isomer is 1-phenyl-*trans*-1,3-butadiene, which is much higher in energy (−8.6 kcal/mol), and the observed laboratory data could not be fit assuming a dominant production of this structure. In the phenyl-d_6-1,3-butadiene system, we found an atomic hydrogen loss from the phenyl group, with the intensity of this channel being 58 ± 15% of that for phenyl-1,3-butadiene. Together with the fact that the two systems could be fit with identical center-of-mass functions this result confirmed that the 1,4-dihydronaphthalene isomer is the prevalent reaction product and that the H atom is most likely split from the phenyl group. In the phenyl-d_5-1,3-butadiene-1,1,4,4-d_4 system, no compelling evidence for an H atom elimination from the C2/C3 atoms of 1,3-butadiene-1,1,4,4-d_4 reactant was found. In the phenyl-d_5-2,3-d_2-1,3-butadiene system, the appearance and intensity of the signal at m/z = 137 was attributed to a hydrogen atom emission from the CH_2 group of the C1 and C4 atoms of 1,3-butadiene-2,3-d_2. A comparison of the absolute intensities of the hydrogen loss from the phenyl group (1,4-dihydronaphthalene) gave the fraction of the H loss from the terminal CH_2 groups of about 32 ± 10%.

These observations are consistent with the reaction mechanism derived from the calculated reaction PES.[38] Here, we found that the phenyl radical adds to a terminal carbon of 1,3-butadiene without a barrier (more precisely, via the formation of a weak van der Waals complex followed by clearance of a submerged barrier leading to a covalently bound $C_6H_5CH_2CHCHCH_2$ adduct). Following a trans−cis rearrangement in the side chain of the initial adduct, a six-member ring closure takes place and then an H loss (from the phenyl group) results in the formation of 1,4-dihydronaphthalene. The highest in energy TS on the pathway to this bicyclic dehydrogenated PAH product resides 16.0 kcal/mol below the initial reactants and 30.1 kcal/mol above the C_6H_5-*trans*-$CH_2CHCHCH_2$ adduct. Alternatively, the adduct can directly lose H from the attacked CH_2 group via a barrier of 41.1 kcal/mol, 5.0 kcal/mol below the reactants, to produce 1-phenyl-*trans*-1,3-butadiene. The formation of 1,4-dihydronaphthalene via this mechanism is also consistent with the experimentally measured $T(\theta)$ angular distribution, which indicated sideways scattering with a maximum at 90° corresponding to a preferential H loss parallel to the total angular momentum vector and almost perpendicularly to the rotational plane of the decomposing intermediate. RRKM calculation of product branching ratios at the zero pressure limit showed the dominance of the 1,4-dihydronaphthalene channel even at the experimental collision energy of 13.1 kcal/mol (93.5% vs 5.8% for 1-phenyl-*trans*-1,3-butadiene). At higher collision energies the $C_6H_5CH_2CHCHCH_2$ formation channel eventually takes over, in agreement with the previous crossed beams experiments at E_{col} = 28.0−38.5 kcal/mol.[89] However, the RRKM calculations clearly overestimated the yield of 1,4-dihydronaphthalene at E_{col} = 13.1 kcal/mol. We attributed this disagreement with experiment to a possible deviation from the statistical behavior under experimental conditions (i.e., a relatively high-energy content of the $C_{10}H_{11}$ intermediates in the absence of collisional deactivation). The dynamical factor should favor the immediate loss of hydrogen from the CH_2 group of 1,3-butadiene forming the non-PAH product.

The de facto barrierless formation of 1,4-dihydronaphthalene via a single collision of C_6H_5 with 1,3-butadiene could be an important step in the formation and of PAH and specifically their partially hydrogenated counterparts in combustion and interstellar chemistry. At flame temperatures 1,4-dihydronaphthalene can be relatively easily dehydrogenated to naphthalene by consecutive loss of two H atoms but the dehydrogenation process will likely be too slow at low temperatures in the ISM or in planetary atmospheres.

Later, we revisited the C_6H_5 + 1,3-butadiene reaction under combustion-like conditions in the high-temperature chemical reactor at 300 Torr and 873 K, where the products were monitored by measuring PIE curves using VUV synchrotron radiation.[39] Here we found the H, CH_3, and C_2H_3 loss product channels with branching ratios evaluated as 86 ± 4%, 8 ± 2%, and 6 ± 2%, respectively. The PIE curves observed for distinct product masses allowed us to assign the following products: three $C_{10}H_{10}$ isomers 1,4-dihydronaphthalene, phenyl-*trans*-1,3-butadiene, and 1-methylindene, three C_9H_8 isomers, indene, phenylallene, and 1-phenyl-1-methylacetylene, and a C_8H_8

DOI: 10.1021/acs.jpca.6b09735
J. Phys. Chem. A 2017, 121, 901−926

isomer, styrene. We concluded that 1,4-dihydronaphthalene, phenyl-*trans*-1,3-butadiene, and styrene are the primary reaction products; here, styrene is produced via phenyl addition to the C2 or C3 atom of 1,3-butadiene via a barrier of 2.9 kcal/mol and the adduct formation is followed by the vinyl group loss from the side chain. Alternatively, the formation of 1-methylindene, indene, phenylallene, and 1-phenyl-1-methylacetylene was attributed to secondary reactions of the phenyl radical with the other three C_4H_6 isomers, 1,2-butadiene, 1-butyne, and 2-butyne, which could be produced by H-assisted isomerization of the initial 1,3-butadiene reactant. In the meantime, the formation of indene from the C_6H_5 + 1,2-butadiene is most likely very minor and not significant enough to be included in kinetic models because indene could not be detected in crossed molecular beam experiments for this reaction[40,42] and was predicted to be only a trace product from theoretical RRKM-ME calculations under combustion conditions.[41] A comparison of the results of crossed molecular beams experiments with those in the chemical reactor allows differentiation between the primary and higher-order reaction products and emphasizes the necessity to consider secondary reactions while describing the processes under combustion-like conditions. In fact, to reproduce the experimental results one needs to compute temperature- and pressure-dependent rate constants for the reactions involved (C_6H_5 + 1,3-butadiene; H-assisted isomerizations of 1,3-butadiene, H + C_4H_6 → products; C_6H_5 + other C_4H_6 isomers, etc.) and then to carry out kinetic modeling of all the reactions together. Such modeling is on our future agenda but beyond the scope of the present work. A successful kinetic model can be then extrapolated from the chemical reactor conditions to the conditions relevant to particular combustion processes.

6. INDENE FORMATION PATHWAYS AND ITS CONVERSION TO NAPHTHALENE (I1−I4, N6)

We discussed a variety of indene formation pathways in a recent publication[37] where we identified the relevant reactions, described their PESs, computed the temperature- and pressure-dependent rate constants in a broad range of combustion conditions and generated rate expressions for kinetic modeling, and compared our theoretical results with experimental measurements in crossed molecular beams and the chemical reactor for the key reactions, such as C_6H_5 + C_3H_4 (allene and propyne)[33,34] and benzyl radical + C_2H_2.[90] Therefore, we only briefly reiterate the main conclusions here.

We found that the reaction of phenyl with allene is fast but directly produces only a small yield of indene, with 3-phenylpropyne predicted as a major product under combustion-relevant conditions. However, 3-phenylpropyne can be converted to indene through a secondary reaction with H radicals:

$$C_6H_5 + \text{allene} \rightarrow \text{indene} + H$$

$$C_6H_5 + \text{allene} \rightarrow \text{3-phenylpropyne} + H$$

$$\text{3-phenylpropyne} + H \rightarrow \text{indene} + H$$

The experimental observation of a large yield of indene in the chemical reactor for the C_6H_5 + allene reaction[33] was attributed to the H-assisted isomerization of non-PAH $C_6H_5C_3H_3$ isomers like 3-phenylpropyne. In the zero-pressure limit, indene was calculated to be the predominant reaction product, in agreement with the results of crossed molecular beams experiments.[34] The C_6H_5 + propyne and C_6H_6 + propargyl reactions do not contribute to the indene synthesis significantly under combustion conditions but the reaction of phenyl with propyne can form indene as the main product at extremely low pressures, as indicated by both crossed beams experiments and RRKM calculations for single-collision conditions.[34]

The reaction of benzyl radical with acetylene,

$$\text{benzyl} + C_2H_2 \rightarrow \text{indene} + H$$

is much slower than C_6H_5 + C_3H_4 but forms indene as the main products in all conditions considered; indene was identified as the exclusive product in the chemical reactor experiment at 600 ± 100 K and 300 Torr.[90] The relative yield of indene in this reaction grows with decreasing temperature and pressure. However, all three C_6H_5 + allene/propyne and C_7H_7 + C_2H_2 reactions are hindered by significant entrance barriers, 2.6, 3.3, and 12.1 kcal/mol, respectively, and hence are expected to be too slow at low temperatures typical for the ISM or Titan's atmosphere.

Another potentially important source of indene in combustion involves the following reaction sequence:

$$C_6H_5 + \text{propene} \rightarrow \text{3-phenylpropene} + H$$

$$\text{3-phenylpropene} + H \rightarrow \text{1-phenylallyl} + H_2$$

$$\text{1-phenylallyl} \rightarrow \text{indene} + H$$

3-Phenylpropene, which is the predominant product of the first reaction at high temperatures, can be activated by H abstraction producing the 1-phenylallyl radical, which unimolecularly decomposes to indene. 1-Phenylallyl can be also produced via the reaction of phenyl with allyl:

$$C_6H_5 + C_3H_5 \rightarrow \text{1-phenylallyl} + H$$

which is barrierless in the entrance channel and 8.0 kcal/mol exoergic overall. 1-Phenylallyl needs to overcome a ∼35 kcal/mol barrier to dissociate to indene and does not survive at temperatures above 1650 and 2000 K at the pressures of 30 Torr and 1 atm, respectively. The calculated lifetime of 1-phenylallyl with respect to its decomposition to indene + H at 1500 K and 1 atm is ∼0.8 μs.

The calculations have shown that indene can be transformed to naphthalene by methylation. For instance, the indenyl + CH_3 reaction can produce 1-methylindenyl and this radical, under typical combustion conditions, can rapidly decompose to the $C_{10}H_8$ isomers, 1-methyleneindene and naphthalene. As discussed above, 1-methyleneindene can be efficiently converted to more stable naphthalene by H-assisted isomerization. We proposed the following PAH growth mechanism involving H abstractions and consecutive additions of methyl radical and acetylene:

$$C_6H_6 + H \rightarrow C_6H_5 + H_2$$

$$C_6H_5 + CH_3 \rightarrow C_6H_5CH_3(\text{toluene}) \rightarrow C_6H_5CH_2(\text{benzyl}) + H$$

$$\text{benzyl} + C_2H_2 \rightarrow \text{indene} + H$$

$$\text{indene} + H \rightarrow \text{indenyl} + H_2$$

$$\text{indenyl} + CH_3 \rightarrow \text{1-methylindenyl} + H$$

$$1-\text{methylindenyl} \rightarrow \text{1-methyleneindene} + H$$

$$\text{1-methyleneindene} + H \rightarrow \text{naphthalene} + H$$

DOI: 10.1021/acs.jpca.6b09735
J. Phys. Chem. A 2017, 121, 901−926

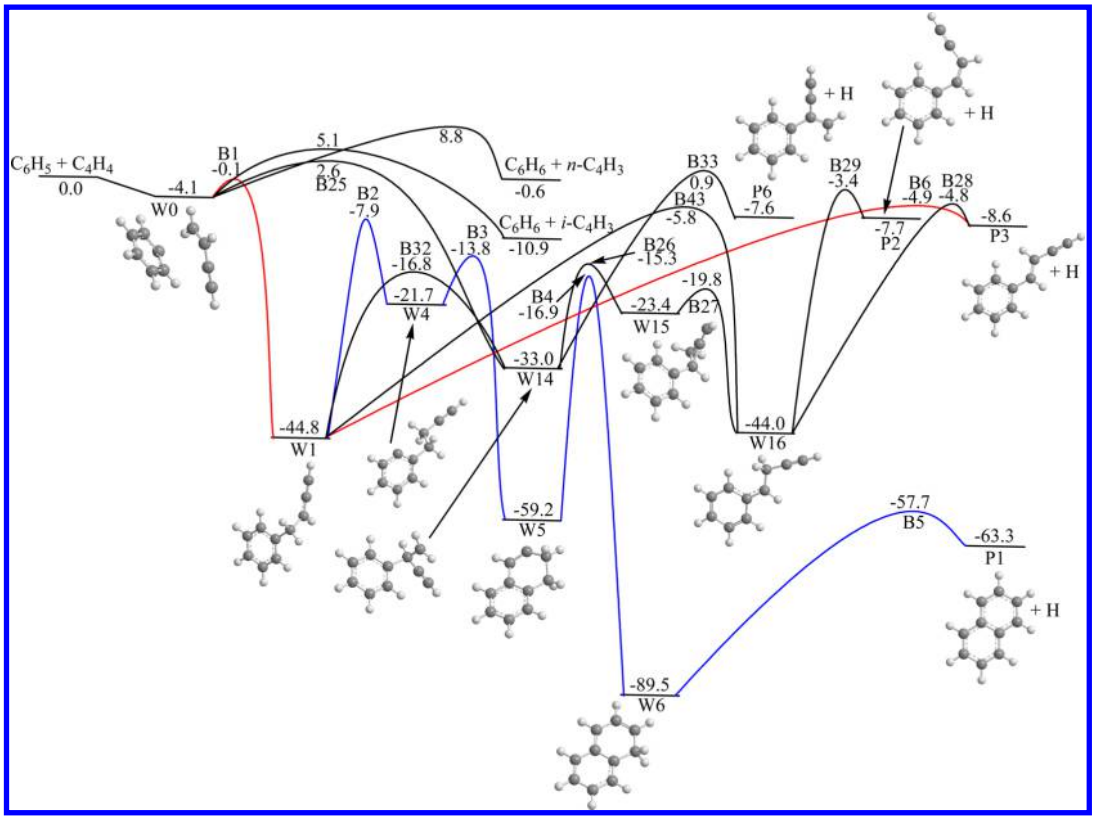

Figure 5. Potential energy diagram for the $C_6H_5 + C_4H_4$ reaction including phenyl addition to vinylic C1 and C2 atoms of vinylacetylene and direct H abstraction pathways. All energies are shown in kcal/mol. Pathways to form naphthalene and *trans*-1-phenylvinylacetylene are shown in blue and red, respectively.

and recommended to include this sequence in kinetic models because first-principle-based rate expressions for most of the reactions are now available.[37,91]

7. $C_6H_5 + C_4H_4$ REACTION (N2)

The reaction of phenyl radical with vinylacetylene has been proposed as a potential source of naphthalene in combustion[14,57,58,61,92] and has been included in the current kinetic models for PAH formation.[93−95] Moriarty and Frenklach[92] first investigated the reaction PES using the density functional B3LYP method and found that the pathways leading to naphthalene via the additions of phenyl to both the triple and double bonds of vinylacetylene should be relatively slow due to high barriers associated with isomerization of the $C_6H_5C_4H_4$ initial adducts by rotation about the double bond or by H migrations preceding the closure of the second six-member ring. They concluded that the pathways to naphthalene cannot compete with the H loss from the initial adducts leading to non-PAH $C_6H_5C_4H_3$ isomers. Alternatively, they proposed that at the second reaction step, H addition to the $C_6H_5C_4H_3$ isomers formed at the first step can produce naphthalene and the reaction rate evaluated for this pathway using time-dependent solution of master equations was found to be close to the value obtained from flame simulations. Moriarty and Frenklach suggested that the two-step mechanism rather than the direct chemically activated path from $C_6H_5 + C_4H_4$ to naphthalene may play a significant role in flame modeling of aromatic growth. However, because the barrier heights for H loss pathways from $C_6H_5C_4H_4$ and for isomerization of these intermediates appeared to be close, relying only on the B3LYP energetics to predict the reaction outcome may not be sufficient.

Aguilera-Iparraguirre and Klopper[96] revisited the $C_6H_5 + C_4H_4$ reaction employing B3LYP and BMK density functional calculations and proposed a new reaction pathway following phenyl addition to the triple bond. In this pathway, a cis−trans isomerization of the side chain occurs via a radical four-member ring intermediate rather than by rotation about the double bond and the corresponding barrier for the former process is lower than for the latter. They validated the BMK/TVZP energetics for this particular pathway vs CCSD(T)/cc-pVTZ results for a smaller analogous system and concluded that the BMK functional provides reasonable accuracy. Next, they used TST to compute high-pressure limit rate constants for individual reaction steps and deduced that the reaction represents a feasible route to naphthalene. However, Aguilera-Iparraguirre and Klopper have not considered the alternative H loss channels and, therefore, the competitiveness of the naphthalene pathway as compared to the production of non-PAH $C_6H_5C_4H_3$ isomers was not established. The pressure effect on the rate constants and relative yield of various products also was not investigated.

The only direct experimental evidence that the phenyl + vinylacetylene reaction can indeed synthesize naphthalene comes from our work in which we combined crossed molecular beam measurements with a more detailed higher-level theoretical study of the PES.[44] In this paper, we examined the gas phase reactions of phenyl and its d_5-substituted isotopomer with C_4H_4 under single collision conditions (approaching zero-pressure) by perpendicularly intersecting supersonic beams of phenyl and phenyl-d_5 radicals with

DOI: 10.1021/acs.jpca.6b09735
J. Phys. Chem. A 2017, 121, 901−926

vinylacetylene at collision energies of ∼11 kcal/mol. The neutral reaction products were ionized by electron impact and then detected in a quadrupole mass spectrometer, which recorded time-of-flight (TOF) spectra of the ionized products. According to the reactive scattering signal at m/z = 128, a $C_{10}H_8$ product (+H) of the C_6H_5 + C_4H_4 of a single-collision event was identified but no $C_{10}H_9$. The C_6D_5 + C_4H_4 reaction under identical conditions formed the product with m/z = 133 ($C_{10}H_3D_5^+$), indicating that the hydrogen atom splits predominantly from the vinylacetylene moiety rather than from the phenyl group. The best fits of the laboratory TOF spectra allowed us to deduce the center-of-mass angular $T(\theta)$ and translational flux distributions $P(E_T)$. It appeared that the laboratory data for both C_6H_5/C_6D_5 + C_4H_4 reactions could be fit with identical center-of-mass functions corresponding to a single channel with the mass combinations of 128 ($C_{10}H_8$) plus 1 (H) and 133 ($C_{10}D_5H_3$) plus 1 (H). The high-energy cutoff of the $P(E_T)$ distribution, which gives the sum of the reaction exoergicity and the collision energy for the molecules formed without internal excitation, was found at 75.3 ± 7.2 kcal/mol, suggesting that at least one of the reaction products is exoergic by 64.1 ± 7.2 kcal/mol. This product could be only naphthalene, for which the G3(MP2,CC)//B3LYP computed reaction energy is −63.3 kcal/mol, but could not be any of the non-PAH vinylphenyl (phenylvinyl)acetylene isomers, which are predicted to be exoergic only by 2.2−10.0 kcal/mol.

The PES calculations helped to unravel the reaction mechanism to produce naphthalene. They showed that the most favorable pathway proceeds via phenyl addition to the terminal vinylic carbon atom C1 to the adduct W1 (Figure 5), which is then subjected to an H atom shift from the ortho position in the ring to the β-C atom of the side chain leading to W4. The latter intermediate undergoes a six-member ring closure to W5. Another H migration from a CH_2 group in the newly formed ring to the adjacent bare carbon atom produces the 1*H*-naphthyl radical, which then splits the extra hydrogen atom to form naphthalene (P1) via an exit barrier of 5.6 kcal/mol. The highest in energy TS along this reaction pathway, B2, corresponds to the H shift from the ring to the side chain and resides 7.9 kcal/mol below the initial reactants. The W1 → W4 isomerization is expected to compete with the H loss from W1 leading to the P3 product, *trans*-1-phenylvinylacetylene, via TS B6, 3.4 kcal/mol lower in energy than the reactants. The C_6H_5/C_6D_5 + C_4H_4 → W1 → W4 → W5 → W6 → P1 + H route to naphthalene is consistent with the experimental observations: first, the calculated reaction exoergicity closely matches the value predicted from the measured high-energy cutoff of $P(E_T)$; second, this mechanism is consistent with the H loss from the vinylacetylene reactant (actually, from the C1 atom) deduced from the isotope substitution experiment. Third, the computed exit barrier height for the H loss is close to the observed pronounced distribution maximum of 7.2−9.6 kcal/mol in the $P(E_T)$ pointing at a tight exit TS. Finally, the $T(\theta)$ distribution exhibits a distinct maximum at 90° corresponding to predominantly sideways scattering that reveals particular geometrical constraints for the dissociating $C_{10}H_9/C_{10}H_4D_5$ intermediates. The hydrogen atom has to be ejected almost parallel to the total angular momentum vector and perpendicularly to the molecular plane of the rotating, decomposing complex; these constraints are fulfilled in the corresponding H loss TS B5.

A peculiar feature of this pathway to naphthalene is that all TSs lie lower in energy than the reactants. When phenyl approaches the C1 atom of C_4H_4, the PES exhibits an attractive behavior and the minimal energy reaction path (MEP) leads to a van-der-Waals complex W0. After the complex is formed, the further approach results in the formation of a covalently bound intermediate W1 via a tight TS B1, which lies lower in energy than the separated reactants. Thus, the addition of phenyl to C1 occurs via a submerged barrier and the overall reaction C_6H_5 + C_4H_4 → W1 is de facto barrierless. In our previous work,[44] the existence of the van-der-Waals complex and the submerged barrier was verified by CASPT2(7,7)/6-311G**//CASSCF(9,9)/6-311G** + ZPE(CASSCF(9,9)/6-311G**) calculations of the entrance channel potential energy curve along the MEP. We attributed this barrierless character of phenyl addition to vinyl acetylene to two factors, the enhanced polarizability of vinylacetylene of 7.70 Å^3 resulting in stronger attractive long-range dispersion forces between phenyl and vinylacetylene compared to that between phenyl and acetylene (3.48 Å^3) or ethylene (4.15 Å^3), and a relatively low difference of the ionization energy (IE) of the molecule (vinylacetylene) and electron affinity (EA) of the radical reactant (phenyl). Here, IE − EA was computed to be 8.48 eV, i.e., below 8.75 eV, the value was proposed in the literature[97] as a semiempirical criterion for a reaction between an unsaturated hydrocarbon with an open shell reactant to be barrierless and fast at low temperatures.

We used RRKM theory to compute energy-dependent rate constants for unimolecular reaction steps starting from chemically activated $C_6H_5C_4H_4$ adducts for various collision energies assuming that the collision energy is fully converted into the internal energy of the adducts. This allowed us to derive product branching ratios for zero-pressure conditions corresponding to crossed molecular beam experiments. The results showed that at collision energies below 1.2 kcal/mol, the C_6H_5 + C_4H_4 reaction produces naphthalene nearly exclusively, but at higher collision energies, 1.2−12 kcal/mol, the yield of naphthalene gradually drops, whereas the yield of the non-PAH C_6H_5 products, such as *cis*/*trans*-1-phenylvinylacetylene and 4-phenylvinylacetylene increases to 13−15%. The combined experimental and theoretical study of the phenyl plus vinylacetylene reaction allowed us to conclude that this reaction may represent a facile route to naphthalene in low-temperature/low-pressure astrochemical environments, even including molecular clouds with temperatures down to 10 K. We also speculated that similar reactions of naphthyl radicals with vinylacetylene may produce phenanthrene and anthracene in very low temperature conditions and thus the vinylacetylene addition to a PAH radical may represent a feasible step for PAH growth in harsh astrochemical conditions. We thus concluded that PAHs can grow via vinylacetylene addition reactions even under conditions prevailing in cold molecular clouds and challenged conventional wisdom that PAHs can only be formed at elevated temperatures, such as in combustion flames on Earth or in circumstellar envelopes of evolved carbon stars.

In the meantime, our study was carried out experimentally only at nearly zero-pressure conditions and at a high collision energy of ∼11 kcal/mol and theoretical calculations were performed only at zero pressure and did not consider possible collisional or radiative stabilization of the $C_6H_5C_4H_4$ intermediates. We have not determined the relative yield of naphthalene and the other non-PAH products as a function of temperature and pressure. Neither did we evaluate the absolute reaction rate constants and rate constants for the formation of individual products at different temperatures and

DOI: 10.1021/acs.jpca.6b09735
J. Phys. Chem. A 2017, 121, 901−926

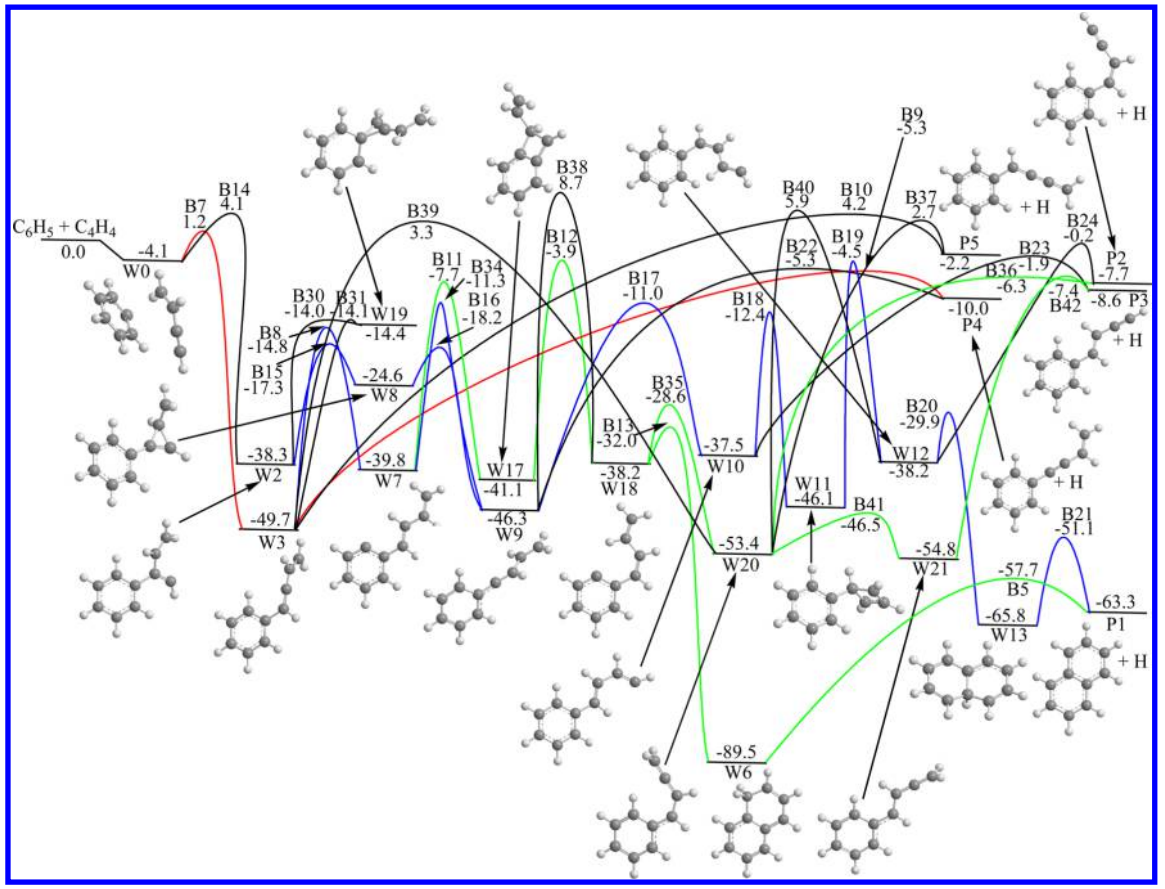

Figure 6. Potential energy diagram for the C_6H_5 + C_4H_4 reaction including phenyl addition to acetylene C3 and C4 atoms of vinylacetylene. All energies are shown in kcal/mol. Pathways to form naphthalene and 4-phenylvinylacetylene are shown in blue and red, respectively. Green curves denote pathways related to the secondary reactions of *trans*- and *cis*-1-phenylvinyaletylene with an H atom.

pressures. Therefore, the previous study could not address such important questions as what are the particular conditions under which the C_6H_5 + C_4H_4 reactions would actually produce naphthalene and in what proportion compared to the other products. With a more detailed PES in hand and with the tool to compute temperature- and pressure-dependent rate constant available (the RRKM-ME approach implemented in the MESS package), we are now able to address these questions.

First of all, we reconsider the existence of the van-der-Waals complex W0 and the submerged barrier for the phenyl addition to C1 to form W1 at a somewhat higher level of theory than in the previous study. Here, we reoptimized geometries of the reactants, the complex W0, and the addition TS B1 using a more accurate double-hybrid B2PLYPD3 functional,[98−100] which includes the D3 correction for a better description of dispersion, with the same 6-311G(d,p) basis set. Single-point energies were then refined at the G3(MP2,CC) level with B2PLYPD3/6-311G(d,p) ZPE. We find that both W0 and B1 at this level of theory still reside lower in energy than the reactants, by 4.1 and 0.3 kcal/mol, respectively. To pinpoint the location and the relative energy of B1, we further performed G3(MP2,CC)//B2PLYPD3/6-311G(d,p) IRCMax calculations;[101] i.e., single-point G3(MP2,CC) energy calculations were carried out for several structures along the MEP obtained from intrinsic reaction coordinate (IRC) calculations at the B2PLYPD3 level. This approach in fact approximates geometry optimization of the TS at the G3(MP2,CC) level. At the IRCMax level the TS position shifts to a shorter C−C distance for the forming bond, from 2.51 Å at the B2PLYPD3 level to 2.45 Å, but the relative energy of B1 changes very little, from −0.34 to −0.25 kcal/mol. Thus, the main conclusion that the critical TS is lower in energy than the reactants is corroborated by the higher level calculations.

We have also performed a more comprehensive study of feasible reaction intermediates, transition states, and bimolecular products, which can be accessed by the phenyl + vinylacetylene reaction; our reaction kinetics scheme reported here includes 22 $C_6H_5C_4H_4$ intermediates, 45 TSs (including 2 direct H abstraction TSs), and 9 bimolecular pairs. The calculated potential energy diagrams are depicted in Figure 5 (phenyl addition to the double bond and direct H abstraction pathways) and Figure 6 (phenyl addition to the triple bond routes). Let us consider first the double bond addition pathways. As described above, after phenyl addition to C1 forming the $C_6H_5CH_2CHCCH$ adduct W1 the reaction proceeds by 1,4-H migration from the ring to the side chain giving $C_6H_4CH_2CH_2CCH$ W4, the by ring closure to W5, H migration in the newly formed ring producing 1*H*-naphthyl W6, which finally splits an H atom to yield naphthalene. Alternatively, W1 can directly dissociate to *trans*-1-phenylvinylacetylene P3 via TS B6; IRC calculations confirm that it is the trans-isomer that is formed by an H loss from the CH_2 group in W1. B6 lies only 3.0 kcal/mol above B2, the highest in energy transition state on the path to naphthalene. Clearly, the H loss route from W1 is more favorable in terms of entropy and we will see from the kinetic calculations that the formation of P3 becomes preferable at higher temperatures. Phenyl can also add to C2 via TS B25 residing 2.6 kcal/mol above the reactants.

DOI: 10.1021/acs.jpca.6b09735
J. Phys. Chem. A 2017, 121, 901−926

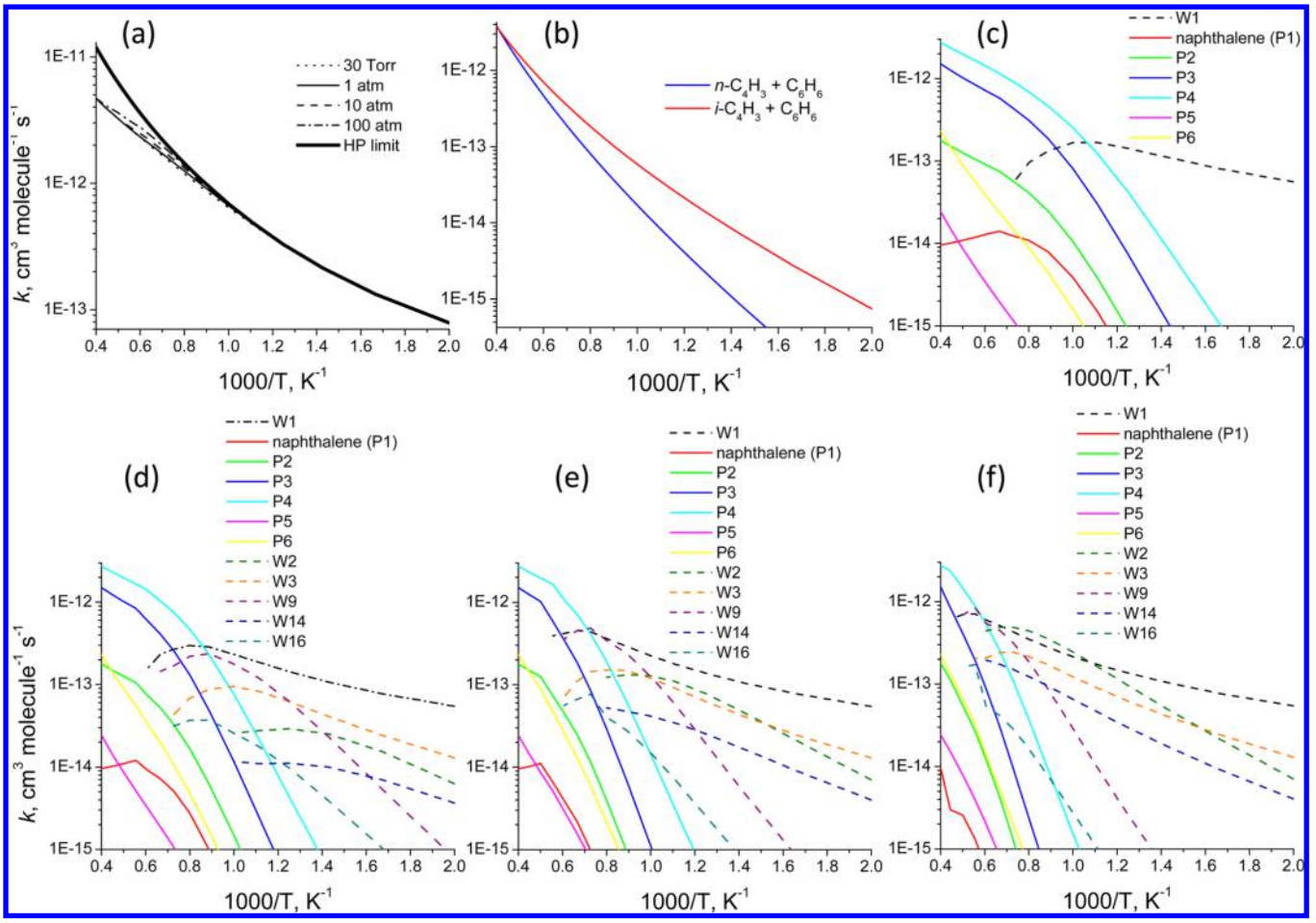

Figure 7. Calculated rate constants for the C_6H_5 + C_4H_4 reaction. (a) shows total addition rate constants at various pressures. (b) shows direct H abstraction rate constants. (c)−(f) show rate constants for the formation of individual products in the addition channels at pressures of 30 Torr and 1, 10, and 100 atm, respectively. See Figures 5 and 6 for the notation of products and intermediates.

As a result, a branched W14 adduct is formed, which can rearrange to W1 by migration of the phenyl moiety over the double bond. Therefore, the two double bond addition pathways are connected. W14 can dissociate to 2-phenylvinylacetylene P6 or undergo a three-member ring closure and opening leading to the intermediate W16, $C_6H_5CHCH_2CCH$, via W15. W16 is also linked to W1 by a 1,2-H shift but the corresponding barrier is much higher than the barriers in the W1 → W14 → W15 → W16 sequence. W16 can split one of the H atoms in the CH_2 to produce either cis- or trans-isomers of 1-phenylvinylacetylene, P2 or P3. The direct H abstractions from vinylacetylene by phenyl lead to the formation of benzene together with *i*- or *n*-C_4H_3 radicals via barriers of 5.1 and 8.8 kcal/mol, respectively.

Next, we look at the triple bond addition pathways (Figure 6). Phenyl addition to the acetylene carbons C3 and C4 lead to a branched adduct W2 and to $C_6H_5CHCCHCH_2$ W3 via barriers of 4.1 and 1.2 kcal/mol, respectively. W2 and W3 can rearrange to one another by migration of the phenyl group over the former triple bond via a metastable intermediate W19 containing a three-member ring; W19 is separated from W2 and W3 by tiny barriers B30 and B31 of 0.4 and 0.3 kcal/mol and is positioned 23.9 and 35.3 kcal/mol above W2 and W3, respectively. W3 is more likely to be formed in the phenyl plus vinylacetylene reaction than W2 due to the lower entrance barrier and we begin from consideration of its isomerization and dissociation pathways. The dissociation channel most favorable energetically is H loss from the α-C atom in the side chain producing 4-phenylvinylacetylene P4 over a barrier of 44.4 kcal/mol at B9. The other H loss from γ-carbon gives phenylbutatriene P5 but the corresponding barrier at B10 is higher, 53.9 kcal/mol. The pathways leading from W3 to naphthalene are complex and multistep: (i) the W3 → H shift from an ortho C atom in the ring to the β-carbon in the side chain → W7 → H shift back to the ring from the α position in the side chain → W9 → 1,4-H migration from the terminal side chain CH_2 group to the α-C → W10 → four-member ring closure → W11 → four-member ring opening →W12 → six-member ring closure → W13 (8a*H*-naphthyl radical) → H loss → naphthalene (P1) + H; and (ii) W3 → W7 → four-member ring closure → W17 → four-member ring opening → W18 → six-member ring closure → W6 (1*H*-naphthyl) → H loss → naphthalene + H. From the intermediate W2, the system can merge onto pathways (i) and (ii) not only at W19 but also via W2 → W8 → W9, which is the rearrangement involving migration of the vinyl group over the former triple bond in vinylacetylene. The highest in energy TSs along pathways (i) and (ii) are B19 and B12 lying 4.5 and 3.9 kcal/mol lower in energy than the initial reactants, respectively. Thus, these TSs are not only slightly higher in energy than the TS B9 (−5.3 kcal/mol) for H loss from W3 but are also above the TS B22 (−5.3 kcal/mol) for H loss from W9 to form 4-phenyl-

DOI: 10.1021/acs.jpca.6b09735
J. Phys. Chem. A 2017, 121, 901−926

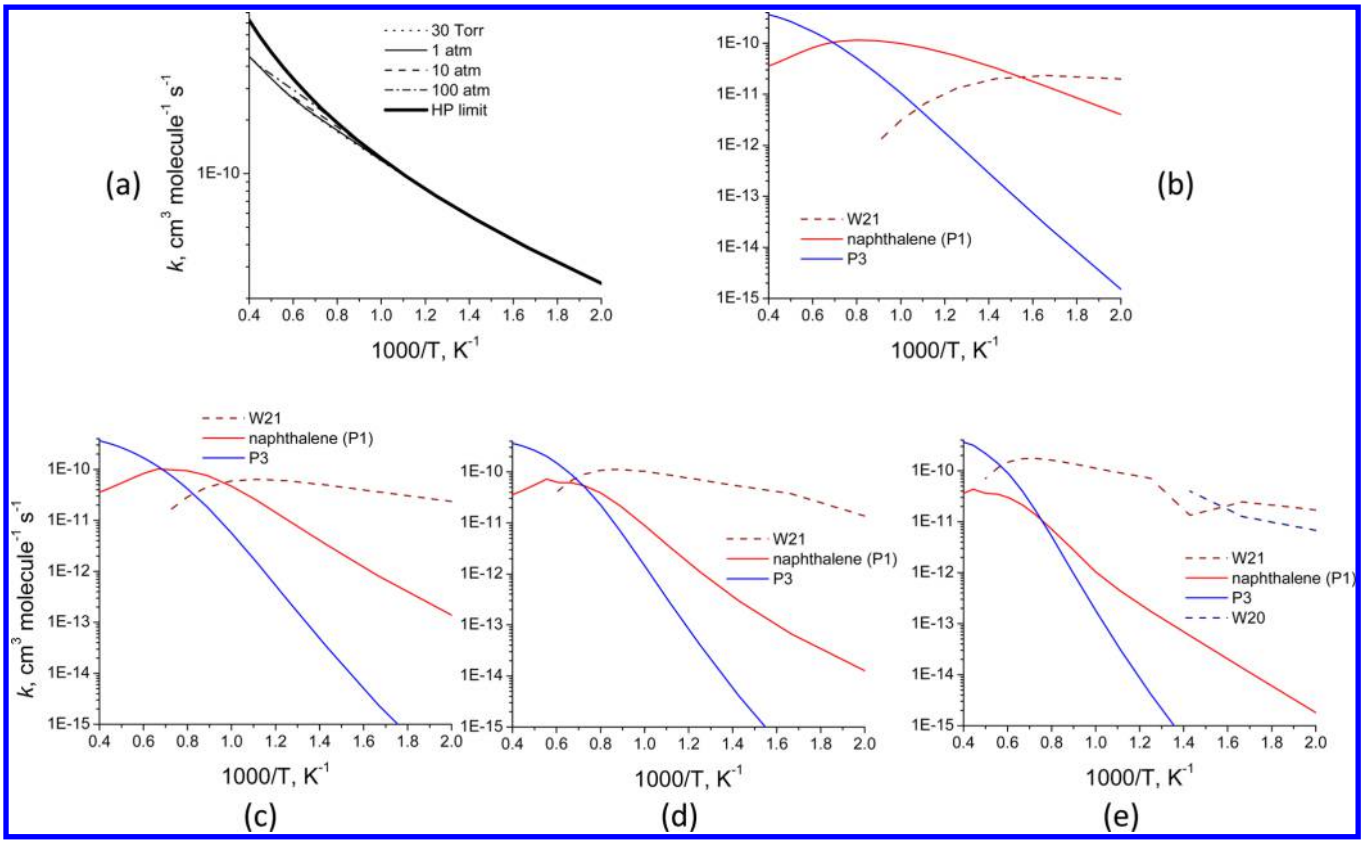

Figure 8. Calculated rate constants for the *cis*-1-phenylvinylacetylene (P2) + H reaction. (a) shows total rate constants at various pressures. (b)−(e) show rate constants for the formation of individual products at pressures of 30 Torr and 1, 10, and 100 atm, respectively. See Figures 5 and 6 for the notation of products and intermediates.

vinylacetylene P4. We anticipate therefore the formation of naphthalene from W2 and W3 would be overtaken by the H loss channels producing P4, especially as the temperature rises increasing the significance of the entropic factor. The other possible products of dissociation of W2 and W3 include *cis*- and *trans*-1-phenylvinylacetylenes (P2 and P3), which can be formed by H losses from W12, W20 and W10, W21, respectively. Noteworthy, the lowest barrier pathways for the reverse reactions P2 + H and P3 + H lead to W20 and W21 ($C_6H_5CHCHCCH_2$), which easily interconvert to one another by rotation around a C−C bond. Next, W20 can undergo a 1,5-H shift from the ortho carbon in the ring leading to W18, six-member ring closure to W6, and H loss to naphthalene. We will see the implications of the existence of this facile pathway to the outcome of the 1-phenylvinylacetylene + H reactions.

We first address the C_6H_5 + C_4H_4 total reaction and product formation rate constants under combustion conditions. The total reaction rate constants in the temperature range 500−2500 K at pressures of 30 Torr and 1, 10, and 100 atm, and at the high-pressure limit (HP) are illustrated in Figure 7a. The calculated rate constants are relatively high and increase from 7.8×10^{-14} to 4.7×10^{-12} cm^3 molecule^{-1} s^{-1} with temperature at finite pressure. The only experimental measurement of the total rate constant for C_6H_5 + C_4H_4 was reported by Yu and Lin and their value, $(7.99 \pm 2.99) \times 10^{-15}$ cm^3 molecule^{-1} s^{-1} at 297 K,[102] is about a factor of 3 lower than our value calculated here, 2.5×10^{-14} cm^3 molecule^{-1} s^{-1}. The falloff behavior of the rate constants is predicted to be rather modest; at the largest deviation of the finite-pressure rate constants from the HP value is a factor of 2.54 at 2500 K where all rate constants in the pressure range of 30 Torr to 100 atm converge. The highest ratio k(100 atm)/k(30 Torr) = 1.21 is found at 1500 K. Pressure-independent direct H abstraction rate constants for the production of *i*-C_4H_3 and *n*-C_4H_3 are illustrated in Figure 7b. Due to substantial barriers of 5.1 and 8.8 kcal/mol, respectively, the H abstraction channels are generally slower than the addition channels, but their significance rises with temperature. For instance, the k_{abs}(*i*-C_4H_3)/k_{add}(total) and k_{abs}(*n*-C_4H_3)/k_{add}(total) ratios increase from 0.09 and 0.03 at 1000 K to 0.13 and 0.23 at 1500 K, to 0.47 and 0.39 at 2000 K, and to 0.80 and 0.81 at 2500 K, respectively.

Although the pressure dependence of the total addition rate constants is not strong, the opposite is true for rate constants for individual product channels and hence for product branching ratios (Figure 7c−f). At 30 Torr, collisional stabilization of the initial adduct W1 persists up to 1375 K and it remains the prevailing product at $T \leq 900$ K. At higher temperatures, the formation of the bimolecular products, 4-phenylvinylacetylene (P4) + H and *trans*-1-phenylvinylacetylene (P3) + H, becomes dominant, with their branching ratios being 40−58% and 13−32%, respectively, at T = 1000−2500 K. At higher pressures W1 still exists as a product up to 1650 K (1 atm), 1800 (10 atm), and 2250 K (100 atm) and additionally the yields of W3, W2, W9, W14, and W16 become noticeable, but P4 and P3 remain the predominant bimolecular products. The other bimolecular products are minor; the branching ratios of *cis*-1-phenylvinylacetylene (P2) and 2-phenylvinylacetylene do not exceed 4−5% with the maximal values reached at 2500 K and those of naphthalene (P1) and phenylbutatriene (P5)

DOI: 10.1021/acs.jpca.6b09735
J. Phys. Chem. A 2017, 121, 901−926

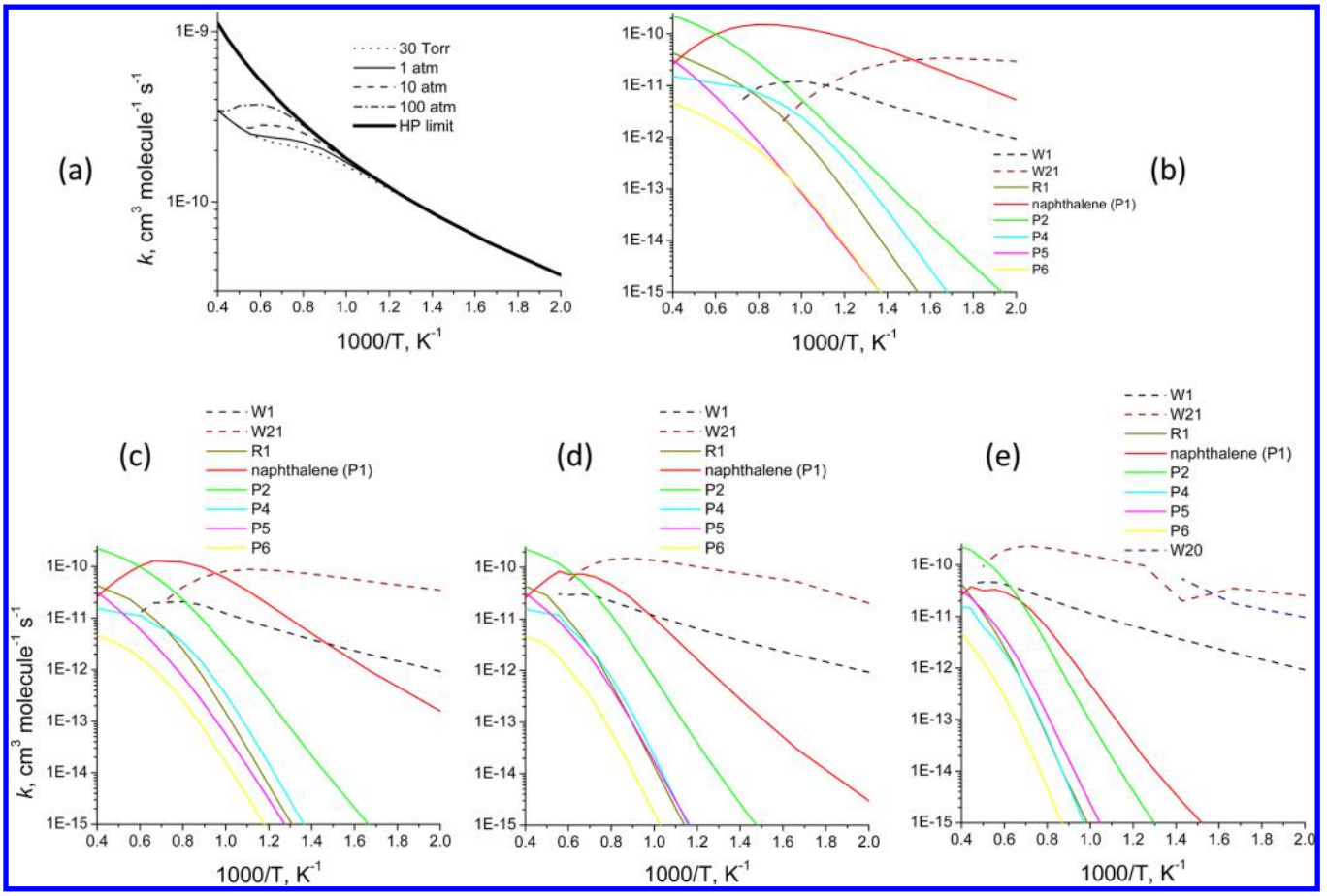

Figure 9. Calculated rate constants for the *trans*-1-phenylvinylacetylene (P3) + H reaction. (a) shows total rate constants at various pressures. (b)−(e) show rate constants for the formation of individual products at pressures of 30 Torr and 1, 10, and 100 atm, respectively. See Figures 5 and 6 for the notation of products and intermediates.

are only fractions of 1%. Clearly, under combustion conditions, naphthalene can be considered only as a trace product of the phenyl plus vinylacetylene reaction. At T = 1500 K and p = 1 atm typical for combustion flames, the C_6H_5 + C_4H_4 → naphthalene + H rate constant is computed to be as low as 2.05 × 10^{-16} cm^3 $molecule^{-1}$ s^{-1} and the branching ratio for this product channel is only 0.03%. This allows us to conclude that the reaction should not be considered as a direct source of naphthalene in combustion.

Alternatively, secondary reactions of 1-phenylvinylacetylene, the trans-conformation of which is one of the major products of C_6H_5 + C_4H_4, with an H atom, can rapidly and efficiently form naphthalene in a certain range of conditions. Figure 8 shows the total and individual rate constants for the P3 + H reaction. The reaction is computed to be fast, with finite-pressure rate constants being in the range 3.68 × 10^{-11} to 3.46 × 10^{-10} cm^3 $molecule^{-1}$ s^{-1} in the 500−2500 K temperature range. One can see that at 30 Torr naphthalene is the prevailing product of the *trans*-1-phenylvinylacetylene + H reaction at T = 700−1650 K. At lower temperature, collisional stabilization of W21, $C_6H_5CHCHCCH_2$, is more favorable, whereas at higher temperatures *cis*-1-phenylvinylacetylene P2 takes over as the main product. At p = 1 atm, naphthalene prevails in a narrower temperature range of 1125−1650 K and at 10 atm only around 1600 K. At 100 atm, stabilization of intermediates W20 and W1 becomes more favorable and the branching ratio of naphthalene in the P3 + H reaction does not exceed 11% (at 2250 K). Nevertheless, even at high pressures in the temperature range of 1500−2500 K, the calculated P3 + H → naphthalene + H rate constants are relatively high, (2.56−7.38) × 10^{-11} cm^3 $molecule^{-1}$ s^{-1}. Moreover, the reaction product dominant at high temperatures, P2, can be converted to naphthalene through H-assisted isomerization (Figure 9). The total rate constants for the P2 + H reaction grow from 2.44 × 10^{-11} to 4.54 × 10^{-10} at T = 500−2500 K and the main products are W21 at lower temperatures, naphthalene in the middle temperature range (700−1375 and 1125−1375 K at 30 Torr and 1 atm, respectively), and *trans*-1-phenylvinylacetylene at higher temperatures. Above 1500 K, cis- and trans-conformations of 1-phenylvinylacetylene P2 and P3 convert to one another moving toward equilibrium but a significant fraction of them transforms to naphthalene. Therefore, the mechanism for naphthalene formation involving the phenyl plus vinylacetylene reaction under combustion condition can indeed be written as a two-step process, in agreement with the suggestion by Moriarty and Frenklach:[92]

$$C_6H_5 + C_4H_4 \rightarrow P3 + H$$

$$P3 + H \rightarrow \text{naphthalene} + H$$

$$P2 + H \rightarrow \text{naphthalene} + H$$

$$P3 + H \leftrightarrows P2 + H$$

On the contrary, the secondary reaction of 4-phenylvinylacetylene P4 with H is not anticipated to produce a

DOI: 10.1021/acs.jpca.6b09735
J. Phys. Chem. A 2017, 121, 901−926

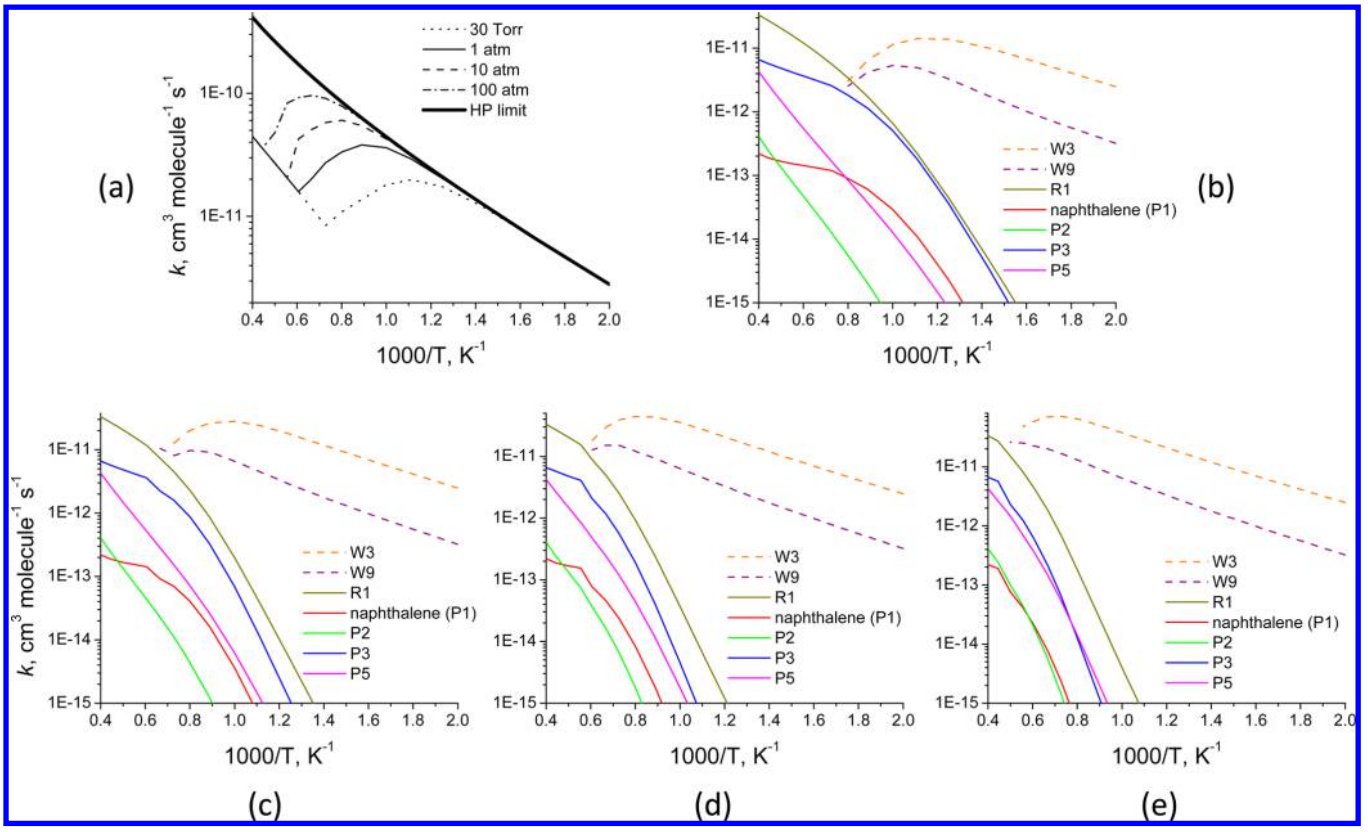

Figure 10. Calculated rate constants for the 4-phenylvinylacetylene (P4) + H reaction. (a) shows total rate constants at various pressures. (b)−(e) show rate constants for the formation of individual products at pressures of 30 Torr and 1, 10, and 100 atm, respectively. See Figures 5 and 6 for the notation of products and intermediates.

significant amount of naphthalene (Figure 10). Interestingly, the total rate constant for this reaction exhibits strong pressure dependence in the 700−2250 K temperature range where the difference between the values at 30 Torr and 100 atm can reach up to 1 order of magnitude. The reaction is dominated by stabilization of W3 and W9 at lower temperatures (up to 1125 K at 30 Torr and up to 2000 K at 100 atm) and at higher temperatures mostly returns the initial reactants C_6H_5 + C_4H_4. Because P4 has a much higher branching ratio in the primary phenyl plus vinylacetylene reaction than P3 (e.g., by factors of 2.5 and 1.8 at 1500 and 2500 K, respectively, at 1 atm), we can conclude that a significant but relatively small fraction of the C_6H_5 + C_4H_4 reactants can be converted to naphthalene through the two-step mechanism discussed here and hence the role of the vinylacetylene addition reaction to phenyl in the formation of naphthalene is probably overstated by the current kinetic models of PAH growth. The prevailing products are likely to be the $C_6H_5C_4H_4$ radicals, especially at higher pressures, and 4-phenylvinylacetylene P4. The radicals are phenyl-substituted analogs of C_4H_5 and they may contribute to the further PAH growth via acetylene addition reactions similar to C_4H_5 + C_2H_2, which are likely to produce biphenyl. P4 in turn may be activated by H abstraction leading to analogs of C_4H_3 and their reactions with C_2H_2 might form the *o*-biphenylyl radical, which then might grow to phenanthrene by the HACA-type acetylene addition.

What are the conditions at which naphthalene can be actually produced in the phenyl plus vinylacetylene reaction? Judging from the results of our crossed beams experiments,[44] a low pressure or maybe nearly zero pressure may be the requirement. Hence, we next consider the product branching ratios at zero-pressure limit. Figure 11a depicts product branching ratios as functions of the collision energy in the bimolecular C_6H_5 + C_4H_4 encounter computed using RRKM theory at zero pressure. The yield of naphthalene is close to 97% at E_{col} = 0 and that of *trans*-1-phenylvinylacetylene is about 3%. As the collision energy rises, the yield of non-PAH $C_6H_5C_4H_3$ steadily increases to 20% for P3 and 46% for 4-phenylvinylacetylene P4 at E_{col} = 11.2 kcal/mol, the collision energy in our crossed beam experiment. Accordingly, the yield of naphthalene drops to ∼33%. However, these calculations have a drawback: they do not take into account radiative stabilization of the $C_6H_5C_4H_4$ intermediates through emission of infrared photons. Using the theoretical approach put forward by Klippenstein and co-workers,[103] we evaluated the rate constant for radiative stabilization of W1 at the temperature corresponding to its vibrational energy content due to chemical activation in the phenyl plus vinylacetylene reaction as 18.3 s^{-1} and this value is on the same order of magnitude as the rate constant for the W1 → W4 isomerization, 23.2 s^{-1}, and is much higher than that for the W1 → P3 dissociation, 0.06 s^{-1}. Therefore, radiative stabilization has to be accounted for.

Hence we carried out RRKM-ME calculations taking radiative stabilization of all $C_6H_5C_4H_4$ intermediates into account; this option is available in the MESS program package. First, the calculations were performed at the zero-pressure limit where the convergence to this limit was achieved at $p = 10^{-15}$ bar. The results are shown in Figure 11b. At 60 K, the lowest temperature at which we were able to achieve numerical convergence in RRKM-ME calculations with MESS, naphthalene (+H) is nearly the exclusive bimolecular product, but its branching ratio is only 21% because W1 (72%) and W16 (6%)

DOI: 10.1021/acs.jpca.6b09735
J. Phys. Chem. A 2017, 121, 901−926

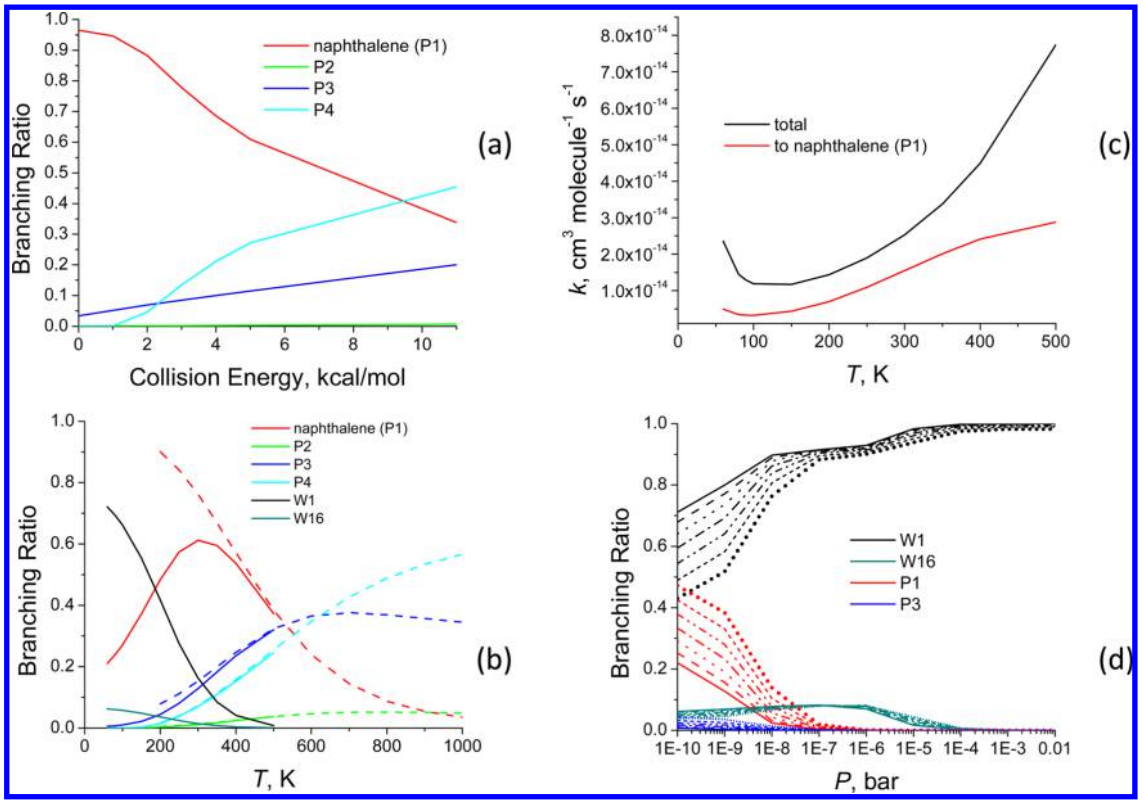

Figure 11. (a) Product branching ratios for the $C_6H_5 + C_4H_4$ reaction calculated for zero pressure and various collision energies using RRKM theory without taking radiative stabilization into account. (b) Branching ratios at the zero-pressure limit calculated using the RRKM-ME approach with MESS with (solid lines) and without (dashed lines) taking radiative stabilization into account. (c) Total and naphthalene formation rate constants of the $C_6H_5 + C_4H_4$ reaction at the zero-pressure limit. (d) Branching ratios as a function of pressure calculated at 80 K (solid lines), 100 K (dashed), 120 K (dotted), 140 K (dash-dotted), 160 K (dash-dot-dotted), 180 K (short dashed), and 200 K (bold dotted). See Figures 5 and 6 for the notation of products and intermediates.

get stabilized radiatively. With increasing temperature radiatiave stabilization plays diminishing roles and the yields of W1 and W6 decrease to nearly zero at 500 and 350 K, respectively. On the contrary, the temperature increase also results in higher yields of non-PAH phenylvinylacetylenes; the branching ratios of P2, P3, and P4 grow to 5%, 35%, and 57%, respectively, at 1000 K. The branching ratio of naphthalene behaves non-monotonically; it reaches its maximum of ~60% at 350 K but then to drops as much as to 3% at 1000 K because of the competition with the non-PAH products P2, P3, and P4. Radiative stabilization is critical at low temperatures but becomes insignificant at 500 K and above. This is observed from the comparison of the calculation results with and without radiative stabilization. If radiative stabilization is not included, the intermediates have to dissociate to dispose the energy of chemical activation and the behavior of the temperature-dependent branching ratios is rather similar to that calculated for collision energy-dependent ones (Figure 11b). At 500 K, the results of calculations without radiative stabilization converge to those with radiative stabilization. Figure 11c shows the calculated total rate constant and that for the $C_6H_5 + C_4H_4 \rightarrow$ naphthalene + H channel in the temperature range of 60−500 K at zero-pressure limit. The total rate constant reaches its minimal value at 150 K and increases at higher and lower temperatures. The rate constant for the naphthalene formation channel exhibits similar behavior but the minimal value is achieved at 100 K. It should be noted that only the inner TS B1 was included in our calculations but at lower temperatures the outer loose TS for the formation of the van-der-Waals complex W0 from the reactants may become rate-determining. However, rate constants for such barrierless processes as $C_6H_5 + C_4H_4 \rightarrow$ W0 are typically in the range of 10^{-10} cm^3 molecule^{-1} s^{-1}, 4 orders of magnitude higher than the values we obtain using the inner TS B1. Hence we do not expect that the outer TS would play a significant role until extremely low temperatures. By simple extrapolation, at low temperatures down to 10 K as prevailing in cold molecular clouds like Taurus Molecular Cloud (TMC-1) the total rate constant of the phenyl plus vinylacetylene reaction and the rate constant for the formation of naphthalene through this reaction at zero-pressure limit can be estimated as $(3-5) \times 10^{-14}$ and $(6-9) \times 10^{-15}$ cm^3 molecule^{-1} s^{-1}, respectively.

Finally, we address pressure dependence of the product branching ratios at low temperatures of 80−200 K in the range of 10^{-10}−10^{-2} bar (Figure 11d). The yield of naphthalene is significant only up to 10^{-8} bar and drops to nearly zero at 10^{-7} bar. The initial adduct W1 becomes the dominant and then exclusive product at higher pressures. Stabilization of another intermediate W16 persists at the level of 5−7% up to 10^{-6} bar but then this product disappears at 10^{-4} bar. The formation naphthalene at very low pressures where it is possible is favored at higher temperatures; for instance, at $p = 10^{-10}$ bar the branching ratios of P1 and W1 are 22% and 71% at 80 K but change to 47% and 43%, respectively, at 200 K. On the basis of this analysis, the $C_6H_5 + C_4H_4$ reaction is not anticipated to produce naphthalene in the PAH forming region of Titan's atmosphere between the altitudes of 140 to 300 km above the surface,[104] where the pressures range from 3×10^{-3} to 10^{-4} bar

DOI: 10.1021/acs.jpca.6b09735
J. Phys. Chem. A 2017, 121, 901−926

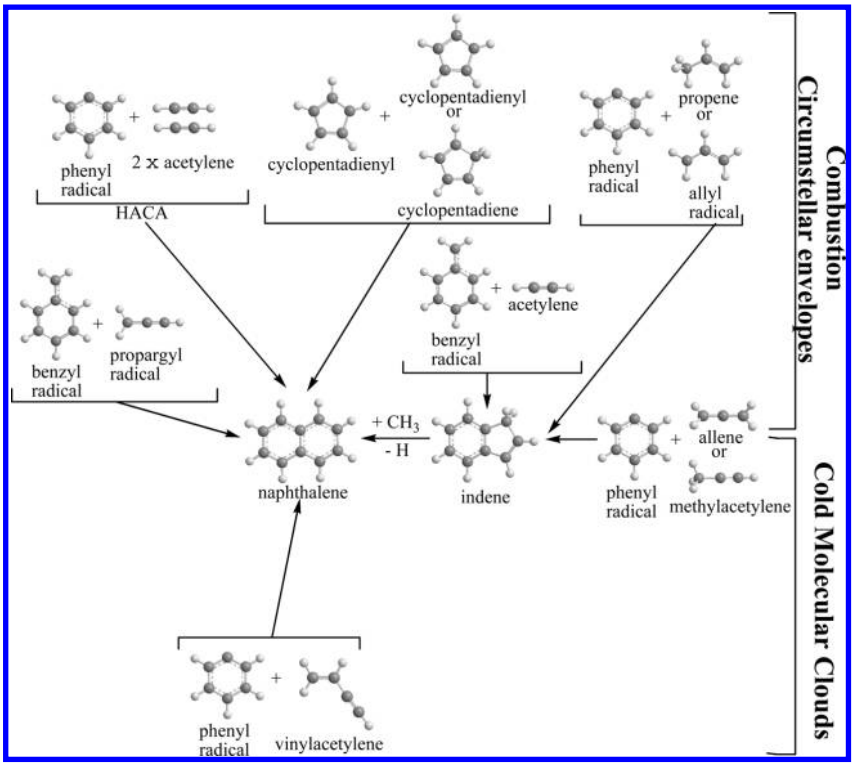

Figure 12. Summary of reaction mechanisms for the formation of naphthalene and indene in combustion and astrochemistry.

with $T \approx 160-180$ K.[105] This region appears to be too dense for naphthalene formation and the reaction would yield the $C_6H_5CH_2CHCCH$ radical W1.

In summary, the formation of naphthalene from C_6H_5 + C_4H_4 in harsh astrochemical conditions is feasible only at extremely low pressures (below 10^{-8} bar) even at temperatures typical for cold molecular clouds but is favored at higher temperatures up to 300 K. These conditions are emulated in crossed molecular beam experiments, where naphthalene was actually observed as a result of single collisions of phenyl with vinylacetylene. In combustion flames on Earth, the reaction can produce naphthalene with significant yield only via a two-step mechanism involving the formation of 1-phenylvinylacetylene $C_6H_5CHCHCCH$ followed by its H-assisted isomerization. This peculiar behavior originates from the features of the PES: the existence of one entrance channel with a submerged barrier (phenyl addition to the double bond), a very small difference (3 kcal/mol) in the energies of the TSs critical for the H loss from the initial adduct and its entropically demanding pathway to naphthalene, and the presence of the other competitive entrance channels with relatively low barriers, such as phenyl addition to the triple bond and direct H abstractions, which do not lead to naphthalene but become prevailing as temperature increases.

8. CONCLUDING REMARKS

In this Article, we outlined and reviewed various formation mechanisms for the prototype PAH molecules, naphthalene and indene, which can be considered as general steps for the PAH growth by one extra six- or five-member ring. As summarized in Figure 12, for the formation of naphthalene in combustion conditions the mechanisms include the HACA routes (**N1**), recombination of cyclopentadienyl radical with itself or with cyclopentadiene (**N3**), the reaction of benzyl radical with propargyl (**N4**), conversion of indenyl radical by methylation (**N6**), and the reactions of phenyl radical with vinylacetylene (**N2**), followed by the reactions of its non-PAH products with H atoms, and 1,3-butadiene (**N5**), where the latter produces dihydrogenated naphthalene. In extreme astrochemical conditions, naphthalene, and dihydronaphthalene can be formed in the C_6H_5 + vinylacetylene (**N2**) and C_6H_5 + 1,3-butadiene (**N5**) reactions, respectively. Ethynyl-substituted naphthalenes can be produced via the ethynyl addition mechanism beginning with benzene (in dehydrogenated forms) or with styrene. The formation mechanisms of indene in combustion include the reactions of phenyl radical with C_3H_4 isomers allene and propyne (**I1**) followed by secondary H-assisted isomerization of the primary products, of benzyl radical with acetylene (**I3**), and unimolecular decomposition of 1-phenylallyl radical produced by H abstraction from 3-phenylpropene, which in turn is a product of the C_6H_5 + propene reaction (**I4**). The C_6H_5 + C_3H_4 reactions (**I1**) hindered by entrance barriers can produce indene directly at low and very low pressures but at elevated temperatures.

Classical HACA-type pathways via mechanisms such as the reaction of phenyl and benzyl with two and one acetylene molecules leading to naphthalene (**N1**) and indene (**I3**), respectively, involve significant entrance barriers to reaction thus blocking those reactions from happening in cold molecular clouds such as TMC-1 and OMC-1. However, these pathways are open in hot astrophysical environments such as in circumstellar envelopes of AGB-type carbon stars like IRC +10216 with temperature conditions close to the photosphere of a few 1000 K. On the contrary, the vinylacetylene mediated formation of naphthalene (**N2**) is barrierless and hence can lead to the synthesis of naphthalene in cold molecular clouds. Therefore, this low-temperature/low-pressure PAH formation involving vinylacetylene represents a strong alternative to classical synthetic routes involving HACA-type pathways. The

DOI: 10.1021/acs.jpca.6b09735
J. Phys. Chem. A 2017, 121, 901−926

work presented here is just the beginning to a better understanding of the formation of PAHs in extreme environments. Future experimental and theoretical studies on PAH formation in low- and high-temperature environments should be expended in at least two directions. *First*, PAHs up to coronene have been detected in meteorites such as Murchison, but so far all attempts to clarify their formation routes have failed both experimentally and computationally. Considering the next members in the PAH series (anthracene and phenanthrene) electronic structure calculations[106] suggest that HACA-type pathways such as the reaction of naphthyl radicals with acetylene do not form anthracene and/or phenanthrene but do stop with the formation of acenaphthalene. Recent experiments probing the reaction of 1-naphthyl with acetylene in a pyrolytic reactor verified this conclusion; only acenaphthalene was detected.[107] Therefore, HACA type mechanisms involving two-three ring systems tend to stop with the formation of naphthalene and acenaphthalene but can unlikely be extended to the growth of anthracene and/or phenanthrene. On the contrary, vinylacetylene-type reactions of 1- and 2-naphthyl radicals with vinylacetylene might extend the barrierless pathways of PAH formation from naphthalene to anthracene and/or phenanthrene under low-temperature/low-pressure conditions. These reactions along with the formation of more complex PAHs carrying four and even five six-membered rings shall be studied under single collision conditions in future experiments and should be contemplated by electronic structure calculations. *Second*, very recently, the underlying reaction pathways leading to the formation of nitrogen-substituted PAHs (NPAHs) have begun to emerge.[108] Here, NPAHs could be the key precursors to nucleobases, which are themselves the essential building blocks of fundamental to life molecules RNA and DNA. NPAHs and nucleobases have been found in significant proportions within meteorites and as such been proposed as a key link in the origin of life on Earth through their exogenous delivery. Considering that nitrogen (N) is isoelectronic to methylidyne (CH), reaction routes leading to mass growth and PAH formation might be open to nitrogen bearing systems as well. Recent studies exploiting a pyrolytic reactor revealed indeed that the reaction of pyridyl radicals with acetylene does lead to the formation of (iso)quinoline, the nitrogen-substituted counterparts of naphthalene involving HACA-type reaction pathways.[109] Theoretically, we demonstrated that NPAH can be also formed at low temperatures through consecutive CN and C_2H additions to styrene and *N*-methylenebenzenamine.[110] Therefore, these findings provide new insights into the formation mechanisms of aromatic molecules incorporating nitrogen atoms through gas phase radical mediated reactions in high-temperature circumstellar envelopes, and hopefully in future studies through vinylacetylene- or C_2H/CN-mediated reactions in low-temperature interstellar environments such as in cold molecular clouds.

The experimental and theoretical results discussed in the present work demonstrate very significant pressure dependence for the rate constants, especially the product-channel specific rate constants. Therefore, accurate evaluation of not only temperature- but also pressure-dependent rate constants will be important for meaningful explorations of the role of various pathways to hydrocarbon growth in combustion and astrochemistry. The implication of the strong pressure and temperature dependence of the reaction outcome is that the relative product yields measured experimentally at low pressures in typical flow reactors experiments, low-pressure flame speciation studies, or under single-collision conditions in crossed molecular beams may be very different from the product distribution at atmospheric and higher pressures. Nevertheless, such experiments remain to be of great value in calibrating pressure-dependent models properly. The development of new experimental techniques probing real combustion conditions, such as the pyrolytic chemical reactor combined with product characterization using the analysis of photoionization efficiency curves, is invaluable for further improvement of kinetic models and empowering them with predictive ability.

■ ASSOCIATED CONTENT

Supporting Information

The Supporting Information is available free of charge on the ACS Publications website at DOI: 10.1021/acs.jpca.6b09735.

Input file for RRKM-ME calculations of rate constants of the $C_6H_5 + C_4H_4$ reaction and related reverse reactions using the MESS package and a table listing fitted modified Arrhenius expressions for these reactions appropriate for combustion modeling purposes (PDF)

■ AUTHOR INFORMATION

Corresponding Authors

*A. M. Mebel. E-mail: mebela@fiu.edu.

*R. I. Kaiser. E-mail: ralfk@hawaii.edu.

ORCID

Alexander M. Mebel: 0000-0002-7233-3133

Ralf I. Kaiser: 0000-0002-7233-7206

Notes

The authors declare no competing financial interest.

Biographies

Alexander M. Mebel received his bachelor's degree in physical chemistry at the Moscow Institute of Steel and Alloys and his Ph.D. degree in physical chemistry at Kurnakov's Institute of General and Inorganic Chemistry of Russian Academy of Science in Moscow, Russia. After postdoctoral appointments in Germany, Japan, and the USA, his first faculty position was at the Institute of Atomic and Molecular Sciences (Academia Sinica, Taiwan), and in 2003 he joined the Department of Chemistry and Biochemistry of Florida International University in Miami, Florida, USA, where he is currently Professor of Chemistry. His current research interests include theoretical quantum chemical studies of mechanisms, kinetics, and dynamics of elementary chemical reactions related to combustion, atmospheric, and interstellar chemistry.

DOI: 10.1021/acs.jpca.6b09735
J. Phys. Chem. A 2017, 121, 901−926

Alexander Landera received both his bachelor's degree and his Ph.D. in chemistry, from Florida International University in Miami, Florida, under the direction of Alexander M. Mebel. During his graduate studies, his work centered on the formation of polycyclic aromatic hydrocarbons (PAHs) in astrochemistry and on combustion environments. After graduating, he joined Argonne National Laboratories Chemical Sciences and Engineering division as a postdoctoral appointee, where he studied roaming reactions in small, nitrogen bearing molecules. At Argonne, his advisors are Stephen J. Klippenstein and Lawrence B. Harding. His research interests include chemical reaction kinetics, investigation of gas phase chemical reactions, and reaction dynamics.

Ralf I. Kaiser received his PhD in Chemistry from the University of Münster (Germany) in 1994 and conducted postdoctoral work at UC Berkeley (Department of Chemistry). During 1997−2000 he received a fellowship from the German Research Council (DFG) to perform his Habilitation at the Department of Physics (University of Chemnitz, Germany) and Institute of Atomic and Molecular Sciences (Academia Sinica, Taiwan). He joined the Department of Chemistry at the University of Hawaii at Manoa in 2002, where he is currently Professor of Chemistry and Director of the W. M. Keck Research Laboratory in Astrochemistry. He was elected Fellow of the Royal Astronomical Society, the Royal Society of Chemistry, the American Physical Society, the American Association for the Advancement of Science, and of the Institute of Physics.

■ ACKNOWLEDGMENTS

This work was supported by the U.S. Department of Energy, Basic Energy Sciences DE-FG02-04ER15570 and DE-FG02-03ER15411 to Florida International University and to the University of Hawaii, respectively. A.M.M. acknowledges the Instructional & Research Computing Center (IRCC, http://ircc.fiu.edu) at Florida International University for providing HPC computing resources that have contributed to the research results reported within this paper. We are thankful to Drs. S. J. Klippenstein and Y. Georgievskii for stimulating discussions.

■ REFERENCES

(1) U.S. EPA (Environmental Protection Agency). *Provisional Guidance for Quantitative Risk Assessment of Polycyclic Aromatic Hydrocarbons*; Environmental Criteria and Assessment Office, Office of Health and Environmental Assessment: Cincinnati, OH, 1993.

(2) Dwek, E.; Arendt, R.; Fixsen, D.; Sodroski, T.; Odegard, N.; Weiland, J.; Reach, W.; Hauser, M.; Kelsall, T.; Moseley, S. Detection and Characterization of Cold Interstellar Dust and Polycyclic Aromatic Hydrocarbon Emission, from COBE Observations. *Astrophys. J.* **1997**, *475*, 565−579.

(3) Ehrenfreund, P.; Charnley, S. B. Organic Molecules in the Interstellar Medium, Comets, and Meteorites: A Voyage from Dark Clouds to the Early Earth. *Annu. Rev. Astron. Astrophys.* **2000**, *38*, 427−483.

(4) Ehrenfreund, P.; Sephton, M. A. Carbon Molecules in Space: From Astrochemistry to Astrobiology. *Faraday Discuss.* **2006**, *133*, 277−288.

(5) Duley, W. Polycyclic Aromatic Hydrocarbons, Carbon Nanoparticles and the Diffuse Interstellar Bands. *Faraday Discuss.* **2006**, *133*, 415−425.

(6) Draine, B. T. *Interstellar Dust Grains*. arXiv preprint astro-ph/0304489, 2003.

(7) Tielens, A. G. G. M. Interstellar Polycyclic Aromatic Hydrocarbon Molecules. *Annu. Rev. Astron. Astrophys.* **2008**, *46*, 289−337.

(8) Salama, F. E.; Bakes, L.; Allamandola, A. Tielens, Assessment of the Polycyclic Aromatic Hydrocarbon-Diffuse Interstellar Band Proposal. *Astrophys. J.* **1996**, *458*, 621−636.

(9) Tielens, A. G. *The Physics and Chemistry of the Interstellar Medium*; Cambridge University Press: Cambridge, U.K.,2005.

(10) Ricks, A. M.; Douberly, G. E.; Duncan, M. A. The Infrared Spectrum of Protonated Naphthalene and its Relevance for the Unidentified Infrared Bands. *Astrophys. J.* **2009**, *702*, 301−306.

(11) Spencer, M. K.; Hammond, M. R.; Zare, R. N. Laser Mass Spectrometric Detection of Extraterrestrial Aromatic Molecules: Mini-Review and Examination of Pulsed Heating Effects. *Proc. Natl. Acad. Sci. U. S. A.* **2008**, *105*, 18096−18101.

(12) Pope, C. J.; Miller, J. A. Exploring Old and New Benzene Formation Pathways in Low-Pressure Premixed Flames of Aliphatic Fuels. *Proc. Combust. Inst.* **2000**, *28*, 1519−1527.

(13) Richter, H.; Howard, J. B. Formation of Polycyclic Aromatic Hydrocarbons and their Growth to Soot − A Review of Chemical Reaction Pathways. *Prog. Energy Combust. Sci.* **2000**, *26*, 565−608.

(14) Lindstedt, P.; Maurice, L.; Meyer, M. Thermodynamic and Kinetic Issues in the Formation and Oxidation of Aromatic Species. *Faraday Discuss.* **2001**, *119*, 409−432.

(15) Frenklach, M. Reaction Mechanism of Soot Formation in Flames. *Phys. Chem. Chem. Phys.* **2002**, *4*, 2028−2037.

(16) Mebel, A. M.; Kaiser, R. I. Formation of Resonantly Stabilised Free Radicals via the Reactions of Atomic Carbon, Dicarbon, and Tricarbon with Unsaturated Hydrocarbons: Theory and Crossed Molecular Beams Experiments. *Int. Rev. Phys. Chem.* **2015**, *34*, 461−514.

(17) Gu, X.; Kaiser, R. I. Reaction Dynamics of Phenyl Radicals in Extreme Environments - A Crossed Molecular Beam Study. *Acc. Chem. Res.* **2009**, *42*, 290−302.

(18) Kaiser, R. I. Experimental Investigation on the Formation of Carbon-Bearing Molecules in the Interstellar Medium via Neutral-Neutral Reactions. *Chem. Rev.* **2002**, *102*, 1309−1358.

(19) Kaiser, R. I.; Maksyutenko, P.; Ennis, C.; Zhang, F.; Gu, X.; Krishtal, S. P.; Mebel, A. M.; Kostko, O.; Ahmed, M. Untangling the Chemical Evolution of Titan's Atmosphere and Surface - From Homogeneous to Heterogeneous Chemistry. Faraday Discussion 147: Chemistry of the Planets. *Faraday Discuss.* **2010**, *147*, 429−478.

DOI: 10.1021/acs.jpca.6b09735
J. Phys. Chem. A 2017, 121, 901−926

(20) Gu, X.; Zhang, F.; Guo, Y.; Kaiser, R. I. A Crossed Molecular Beam Study on the Formation of Phenylacetylene from Phenyl Radicals and Acetylene. *Angew. Chem., Int. Ed.* **2007**, *46*, 6866−6869.
(21) Vernon, M. *Thesis*, Univ. California, Berkley, 1981.
(22) Weis, M. S. *Ph.D. Thesis*, Univ. California, Berkley, 1986.
(23) Parker, D. S. N.; Kaiser, R. I.; Kostko, O.; Troy, T. P.; Ahmed, M.; Sun, B.-J.; Chen, S.-H.; Chang, A. H. H. On the Formation of Pyridine in the Interstellar Medium. *Phys. Chem. Chem. Phys.* **2015**, *17*, 32000−32008.
(24) Curtiss, L. A.; Raghavachari, K.; Redfern, P. C.; Rassolov, V.; Pople, J. A. Gaussian-3 (G3) Theory for Molecules Containing First and Second-Row Atoms. *J. Chem. Phys.* **1998**, *109*, 7764−7776.
(25) Curtiss, L. A.; Raghavachari, K.; Redfern, P. C.; Baboul, A. G.; Pople, J. A. Gaussian-3 Theory Using Coupled Cluster Energies. *Chem. Phys. Lett.* **1999**, *314*, 101−107.
(26) Baboul, A. G.; Curtiss, L. A.; Redfern, P. C.; Raghavachari, K. Gaussian-3 Theory Using Density Functional Geometries and Zero-Point Energies. *J. Chem. Phys.* **1999**, *110*, 7650−7657.
(27) Kislov, V. V.; Islamova, N. I.; Kolker, A. M.; Lin, S. H.; Mebel, A. M. Hydrogen Abstraction Acetylene Addition and Diels-Alder Mechanisms of PAH Formation: A Detailed Study Using First Principles Calculations. *J. Chem. Theory Comput.* **2005**, *1*, 908−924.
(28) Mebel, A. M.; Georgievskii, Y.; Jasper, A. W.; Klippenstein, S. J. Temperature- and Pressure-Dependent Rate Coefficients for the HACA Pathways from Benzene to Naphthalene. *Proc. Combust. Inst.* **2016**, DOI: 10.1016/j.proci.2016.07.013.
(29) Kislov, V. V.; Mebel, A. M. The Formation of Naphthalene, Azulene, and Fulvalene from the Recombination Product of Two Cyclopentadienyl Radicals: An Ab Initio/RRKM Study of Rearrangements of the C_5H_5-C_5H_4 (9-H-Fulvalenyl) Radical. *J. Phys. Chem. A* **2007**, *111*, 9532−9543.
(30) Mebel, A. M.; Kislov, V. V. Can the $C_5H_5 + C_5H_5 \rightarrow C_{10}H_{10} \rightarrow C_{10}H_9 + H/C_{10}H_8 + H_2$ Reaction Produce Naphthalene? An Ab Initio/RRKM Study. *J. Phys. Chem. A* **2009**, *113*, 9825−9833.
(31) Kislov, V. V.; Mebel, A. M. An Ab Initio G3-type/Statistical Theory Study of the Formation of Indene in Combustion Flames. II. The Pathways Originated from Reactions of Cyclic C_5 a Species - Cyclopentadiene and Cyclopentadienyl Radical. *J. Phys. Chem. A* **2008**, *112*, 700−716.
(32) Kislov, V. V.; Mebel, A. M. An Ab Initio G3-Type/Statistical Theory Study of the Formation of Indene in Combustion Flames. I. The Pathways Involving Benzene and Phenyl Radical. *J. Phys. Chem. A* **2007**, *111*, 3922−3931.
(33) Zhang, F.; Kaiser, R. I.; Kislov, V. V.; Mebel, A. M.; Golan, A.; Ahmed, M. A VUV Photoionization Study of the Formation of the Indene Molecule and its Isomers. *J. Phys. Chem. Lett.* **2011**, *2*, 1731−1735.
(34) Parker, D. S. N.; Zhang, F.; Kaiser, R. I.; Kislov, V. V.; Mebel, A. M. Indene Formation under Single Collision Conditions from Reaction of Phenyl Radicals with Allene and Methylacetylene − A Crossed Molecular Beam and Ab Initio Study. *Chem. - Asian J.* **2011**, *6*, 3035−3042.
(35) Kaiser, R. I.; Parker, D. S. N.; Goswami, M.; Zhang, F.; Kislov, V. V.; Mebel, A. M.; Aguilera-Iparraguirre, J.; Green, W. H. Crossed Beam Reaction of Phenyl and D5-Phenyl Radicals with Propene and Deuterated Counterparts-Competing Atomic Hydrogen and Methyl Loss Pathways. *Phys. Chem. Chem. Phys.* **2012**, *14*, 720−729.
(36) Kislov, V. V.; Mebel, A. M.; Aguilera-Iparraguirre, J.; Green, W. H. Reaction of Phenyl Radical with Propylene as a Possible Source of Indene and Other Polycyclic Aromatic Hydrocarbons: An Ab Initio/RRKM-ME Study. *J. Phys. Chem. A* **2012**, *116*, 4176−4191.
(37) Mebel, A. M.; Georgievskii, Y.; Jasper, A. W.; Klippenstein, S. J. Pressure Dependent Rate Constants for PAH Growth: Formation of Indene and its Conversion to Naphthalene. *Faraday Discuss.* **2016**, *195*, 637−670.
(38) Kaiser, R. I.; Parker, D. S. N.; Zhang, F.; Landera, A.; Kislov, V. V.; Mebel, A. M. PAH Formation under Single Collision Conditions - Reaction of Phenyl Radical and 1,3-Butadiene to Form 1,4-Dihydronaphthalene. *J. Phys. Chem. A* **2012**, *116*, 4248−4258.
(39) Golan, A.; Ahmed, M.; Mebel, A. M.; Kaiser, R. I. A VUV Photoionization Study on the Formation of Primary and Secondary Products in the Reaction of the Phenyl Radical with 1,3-Butadiene under Combustion Relevant Conditions. *Phys. Chem. Chem. Phys.* **2013**, *15*, 341−347.
(40) Gu, X.; Zhang, F.; Kaiser, R. I.; Kislov, V. V.; Mebel, A. M. Reaction Dynamics of the Phenyl Radical with 1,2-Butadiene. *Chem. Phys. Lett.* **2009**, *474*, 51−56.
(41) Kislov, V. V.; Mebel, A. M. Ab Initio/RRKM-ME Study on the Mechanism and Kinetics of the Reaction of Phenyl Radical with 1,2-Butadiene. *J. Phys. Chem. A* **2010**, *114*, 7682−7692.
(42) Yang, T.; Parker, D. S. N.; Dangi, B. B.; Kaiser, R. I.; Kislov, V. V.; Mebel, A. M. Crossed Beam Reactions of the Phenyl (C_6H_5; X^2A_1) and D5-Phenyl Radical (C_6D_5; X^2A1) with 1,2-Butadiene ($H_2CCCHCH_3$; X^1A'). *J. Phys. Chem. A* **2014**, *118*, 4372−4381.
(43) Kaiser, R. I.; Zhang, F.; Gu, X.; Kislov, V. V.; Mebel, A. M. Reaction Dynamics of the Phenyl Radical (C_6H_5) with 1-Butyne ($HCCC_2H_5$) and 2-Butyne (CH_3CCCH_3). *Chem. Phys. Lett.* **2009**, *481*, 46−53.
(44) Parker, D. S. N.; Zhang, F.; Kim, Y. S.; Kaiser, R. I.; Landera, A.; Kislov, V. V.; Mebel, A. M.; Tielens, A. G. G. M. Low Temperature Formation of Naphthalene and its Role in the Synthesis of PAHs (Polycyclic Aromatic Hydrocarbons) in the Interstellar Medium. *Proc. Natl. Acad. Sci. U. S. A.* **2012**, *109*, 53−58.
(45) Frisch, M. J.; Trucks, G. W.; Schlegel, H. B.; Scuseria, G. E.; Robb, M. A.; Cheeseman, J. R.; Scalmani, G.; Barone, V.; Mennucci, B.; Petersson, G. A.; et al. *Gaussian 09*, Revision A.1; Gaussian, Inc.: Wallingford, CT, 2009.
(46) Werner, H.-J.; Knowles, P. J.; Knizia, G.; Manby, F. R.; Schütz, M.; Celani, P.; Györffy, W.; Kats, D.; Korona, T.; Lindh, R. et al. *MOLPRO*, version 2010.1, a package of ab initio programs, see http://www.molpro.net.
(47) Eyring, H.; Lin, S. H.; Lin, S. M. *Basic Chemical Kinetics*; Wiley: New York, 1980.
(48) Kislov, V. V.; Nguyen, T. L.; Mebel, A. M.; Lin, S. H.; Smith, S. C. Photodissociation of Benzene under Collision-Free Conditions: An Ab Initio RRKM Study. *J. Chem. Phys.* **2004**, *120*, 7008−7017.
(49) Georgievskii, Y.; Miller, J. A.; Burke, M. P.; Klippenstein, S. J. Reformulation and Solution of the Master Equation for Multiple-Well Chemical Reactions. *J. Phys. Chem. A* **2013**, *117*, 12146−12154.
(50) Georgievskii, Y.; Klippenstein, S. J. *MESS Program Package*, 2015, available online at http://tcg.cse.anl.gov/papr.
(51) Klippenstein, S. J.; Miller, J. A.; Jasper, A. W. Kinetics of Propargyl Radical Dissociation. *J. Phys. Chem. A* **2015**, *119*, 7780−7791.
(52) Troe, J. Theory of Thermal Unimolecular Reactions at Low-Pressures. 1. Solutions of Master Equation. *J. Chem. Phys.* **1977**, *66*, 4745−4757.
(53) Jasper, A. W.; Oana, C. M.; Miller, J. A. Third-Body Collision Efficiencies from Combustion Modeling: Hydrocarbons in Atomic and Diatomic Baths. *Proc. Combust. Inst.* **2015**, *35*, 197−204.
(54) Jasper, A. W.; Miller, J. A. Lennard-Jones Parameters for Combustion and Chemical Kinetics Modeling from Full-Dimensaionl Intermolecular Potentials. *Combust. Flame* **2014**, *161*, 101−110.
(55) Frenklach, M.; Clary, D. W.; Gardiner, W. C.; Stein, S. E. Detailed Kinetic Modeling of Soot Formation in Shock-Tube Pyrolysis of Acetylene. *Symp. Combust., [Proc.]* **1985**, *20*, 887−901.
(56) Frenklach, M.; Wang, H. Detailed Modeling of Soot Particle Nucleation and Growth. *Symp. Combust., [Proc.]* **1991**, *23*, 1559−1566.
(57) Wang, H.; Frenklach, M. Calculations of Rate Coefficients for the Chemically Activated Reactions of Acetylene with Vinylic and Aromatic Radicals. *J. Phys. Chem.* **1994**, *98*, 11465−11489.
(58) Appel, J.; Bockhorn, H.; Frenklach, M. Kinetic Modeling of Soot Formation with Detailed Chemistry and Physics: Laminar Premixed Flames of C2 Hydrocarbons. *Combust. Flame* **2000**, *121*, 122−136.
(59) Frenklach, M.; Moriarty, N. W.; Brown, N. J. Hydrogen Migration in Polyaromatic Growth. *Symp. Combust., [Proc.]* **1998**, *27*, 1655−1661.

DOI: 10.1021/acs.jpca.6b09735
J. Phys. Chem. A 2017, 121, 901−926

(60) Moriarty, N. W.; Brown, N. J.; Frenklach, M. Hydrogen Migration in the Phenylethen-2-yl Radical. *J. Phys. Chem. A* **1999**, *103*, 7127−7135.
(61) Bittner, J. D.; Howard, J. B. Composition Profiles and Reaction Mechanisms in a Near-Sooting Premixed Benzene/Oxygen/Argon Flame. *Symp. Combust., [Proc.]* **1981**, *18*, 1105−1116.
(62) Bauschlicher, C. W., Jr.; Ricca, A. Mechanisms for Polycyclic Aromatic Hydrocarbon (PAH) Growth. *Chem. Phys. Lett.* **2000**, *326*, 283−287.
(63) Tokmakov, I. V.; Lin, M. C. Reaction of Phenyl Radicals with Acetylene: Quantum Chemical Investigation of the Mechanism and Master Equation Analysis of the Kinetics. *J. Am. Chem. Soc.* **2003**, *125*, 11397−11408.
(64) Kislov, V. V.; Mebel, A. M.; Lin, S. H. Ab Initio and DFT Study of the Formation Mechanism of Polycyclic Aromatic Hydrocarbons: The Phenanthrene Synthesis from Biphenyl and Naphthalene. *J. Phys. Chem. A* **2002**, *106*, 6171−6182.
(65) Parker, D. S. N.; Kaiser, R. I.; Troy, T. P.; Ahmed, M. Hydrogen Abstraction/Acetylene Addition Revealed. *Angew. Chem., Int. Ed.* **2014**, *53*, 7740−7744.
(66) Yang, T.; Troy, T. P.; Xu, B.; Kostko, O.; Ahmed, M.; Mebel, A. M.; Kaiser, R. I. Hydrogen-Abstraction/Acetylene-Addition Exposed. *Angew. Chem., Int. Ed.* **2016**, *55*, 14983−14987.
(67) Mebel, A. M.; Kislov, V. V.; Kaiser, R. I. On a Photo-Induced Mechanism of the Formation and Growth of Polycyclic Aromatic Hydrocarbons in Low-Temperature Environments via Successive Ethynyl Radical Additions. *J. Am. Chem. Soc.* **2008**, *130*, 13618−13629.
(68) Woon, D. E. Modeling Chemical Growth Processes in Titan's Atmosphere: 1. Theoretical Rates for Reactions Between Benzene and the Ethynyl (C_2H) and Cyano (CN) Radicals at Low Temperature and Pressure. *Chem. Phys.* **2006**, *331*, 67−76.
(69) Landera, A.; Mebel, A. M.; Kaiser, R. I. Theoretical Study of the Reaction Mechanism of Ethynyl Radical with Benzene and Related Reactions on the C_8H_7 Potential Energy Surface. *Chem. Phys. Lett.* **2008**, *459*, 54−59.
(70) Goulay, F.; Leone, S. R. Low-Temperature Rate Coefficients for the Reaction of Ethynyl Radical (C_2H) with Benzene. *J. Phys. Chem. A* **2006**, *110*, 1875−1880.
(71) Jones, B.; Zhang, F.; Maksyutenko, P.; Mebel, A. M.; Kaiser, R. I. Crossed Molecular Beam Study on the Formation of Phenylacetylene and Its Relevance to Titan's Atmosphere. *J. Phys. Chem. A* **2010**, *114*, 5256−5262.
(72) Landera, A.; Kaiser, R. I.; Mebel, A. M. Addition of One and Two Units of C_2H to Styrene: A Theoretical Study of the $C_{10}H_9$ and $C_{12}H_9$ Systems and Implications towards Growth of Polycyclic Aromatic Hydrocarbons at Low Temperatures. *J. Chem. Phys.* **2011**, *134*, 024302.
(73) Dean, A. M. Detailed Kinetic Modeling of Autocatalysis in Methane Pyrolysis. *J. Phys. Chem.* **1990**, *94*, 1432−1439.
(74) Melius, C. F.; Colvin, M. E.; Marinov, N. M.; Pit, W. J.; Senkan, S. M. Reaction Mechanisms in Aromatic Hydrocarbon Formation Involving the C_5H_5 Cyclopentadienyl Moiety. *Symp. Combust., [Proc.]* **1996**, *26*, 685−692.
(75) Marinov, N. M.; Pitz, W. J.; Westbrook, C. K.; Vincitore, A. M.; Castaldi, M. J.; Senkan, S. M.; Melius, C. F. Aromatic and Polycyclic Aromatic Hydrocarbon Formation in a Laminar Premixed n-Butane Flame. *Combust. Flame* **1998**, *114*, 192−213.
(76) Castaldi, M. J.; Marinov, N. M.; Melius, C. F.; Huang, J.; Senkan, S. M.; Pit, W. J.; Westbrook, C. K. Experimental and Modeling Investigation of Aromatic and Polycyclic Aromatic Hydrocarbon Formation in a Premixed Ethylene Flame. *Symp. Combust., [Proc.]* **1996**, *26*, 693−702.
(77) Goldaniga, A.; Faravelli, T.; Ranzi, E. The Kinetic Modeling of Soot Precursors in a Butadiene Flame. *Combust. Flame* **2000**, *122*, 350−358.
(78) Robinson, R. K.; Lindstedt, P. On the Chemical Kinetics of Cyclopentadiene Oxidation. *Combust. Flame* **2011**, *158*, 666−686.
(79) Cavallotti, C.; Polino, D.; Frassoldati, A.; Ranzi, E. Analysis of Some Reaction Pathways Active during Cyclopentadiene Pyrolysis. *J. Phys. Chem. A* **2012**, *116*, 3313−3324.
(80) Cavallotti, C.; Polino, D. On the Kinetics of the C_5H_5 + C_5H_5 Reaction. *Proc. Combust. Inst.* **2013**, *34*, 557−564.
(81) Alder, R. W.; East, S. P.; Harvey, J. N.; Oakley, M. T. The Azulene-to-Naphthalene Rearrangement Revisited: a DFT Study of Intramolecular and Radical-Promoted Mechanisms. *J. Am. Chem. Soc.* **2003**, *125*, 5375−5387.
(82) Wang, D.; Violi, A.; Kim, D. H.; Mullholland, J. A. Formation of Naphthalene, Indene, and Benzene from Cyclopentadiene Pyrolysis: A DFT Study. *J. Phys. Chem. A* **2006**, *110*, 4719−4725.
(83) Colket, M. B.; Seery, D. J. Reaction Mechanisms for Toluene Pyrolysis. *Symp. Combust., [Proc.]* **1994**, *25*, 883−891.
(84) Marinov, N. M.; Pitz, W. J.; Westbrook, C. K.; Lutz, A. E.; Vincitore, A. M.; Senkan, S. M. Chemical Kinetic Modeling of a Methane Opposed-Flow Diffusion Flame and Comparison to Experiments. *Symp. Combust., [Proc.]* **1998**, *27*, 605−613.
(85) D'Anna, A.; Violi, A. A Kinetic Model for the Formation of Aromatic Hydrocarbons in Premixed Laminar Flames. *Symp. Combust., [Proc.]* **1998**, *27*, 425−433.
(86) Blanquart, G.; Pepiot-Desjardins, P.; Pitsch, H. Chemical Mechanism for High Temperature Combustion of Engine Relevant Fuels with Emphasis on Soot Precursors. *Combust. Flame* **2009**, *156*, 588−607.
(87) Zhang, L.; Cai, J.; Zhang, T.; Qi, F. Kinetic Modeling Study of Toluene Pyrolysis at Low Pressure. *Combust. Flame* **2010**, *157*, 1686−1697.
(88) Matsugi, A.; Miyoshi, A. Computational Study on the Recombination Reaction between Benzyl and Propargyl Radicals. *Int. J. Chem. Kinet.* **2012**, *44*, 206−218.
(89) Gu, X.; Zhang, F.; Kaiser, R. I. A Crossed Molecular Beam Study of the Phenyl Radical Reaction with 1,3-Butadiene and its Deuterated Isotopomers. *J. Phys. Chem. A* **2009**, *113*, 998−1006.
(90) Parker, D. S. N.; Kaiser, R. I.; Kostko, O.; Ahmed, M. Selective Formation of Indene through the Reaction of Benzyl Radicals with Acetylene. *ChemPhysChem* **2015**, *16*, 2091−2093.
(91) Klippenstein, S. J.; Harding, L. B.; Georgievskii, Y. On the formation and Decomposition of C_7H_8. *Proc. Combust. Inst.* **2007**, *31*, 221−229.
(92) Moriarty, N. W.; Frenklach, M. Ab Initio Study of Naphthalene Formation by Addition of Vinylacetylene to Phenyl. *Proc. Combust. Inst.* **2000**, *28*, 2563−2568.
(93) Slavinskaya, N. A.; Frank, P. A Modelling Study of Aromatic Soot Precursors Formation in Laminar Methane and Ethene Flames. *Combust. Flame* **2009**, *156*, 1705−1722.
(94) http://web.mit.edu/anish/www/mitsootmodellowpsymp2004.mec.
(95) Shukla, B.; Koshi, M. Comparative Study on the Growth Mechanisms of PAHs. *Combust. Flame* **2011**, *158*, 369−375.
(96) Aguilera-Iparraguirre, J.; Klopper, W. Density Functional Theory Study of the Formation of Naphthalene and Phenanthrene from Reactions of Phenyl with Vinyl- and Phenylacetylene. *J. Chem. Theory Comput.* **2007**, *3*, 139−145.
(97) Smith, I. W. M.; Sage, A. M.; Donahue, N. M.; Herbst, E.; Quan, D. The Temperature-Dependence of Rapid Low Temperature Reactions: Experiment, Understanding and Prediction. *Faraday Discuss.* **2006**, *133*, 137−156.
(98) Grimme, S. Semiempirical Hybrid Density Functional with Perturbative Second-Order Correlation. *J. Chem. Phys.* **2006**, *124*, 034108.
(99) Grimme, S.; Ehrlich, S.; Goerigk, L. Effect of the Damping Function in Dispersion Corrected Density Functional Theory. *J. Comput. Chem.* **2011**, *32*, 1456−1465.
(100) Goerigk, L.; Grimme, S. Efficient and Accurate Double-Hybrid-Meta-GGA Density Functionals—Evaluation with the Extended GMTKN30 Database for General Main Group Thermochemistry, Kinetics, and Noncovalent Interactions. *J. Chem. Theory Comput.* **2011**, *7*, 291−309.

DOI: 10.1021/acs.jpca.6b09735
J. Phys. Chem. A 2017, 121, 901−926

(101) Malick, D. K.; Petersson, G. A.; Montgomery, J. A., Jr. Transition States for Chemical Reactions. I. Geometry and Classical Barrier Height. *J. Chem. Phys.* **1998**, *108*, 5704−5713.
(102) Yu, T.; Lin, M. C. Kinetics of Phenyl Radical Reactions Studied by the "Cavity Ring Down" Method. *J. Am. Chem. Soc.* **1993**, *115*, 4371−4372.
(103) Klippenstein, S. J.; Yang, Y.-C.; Ryzhov, V.; Dunbar, R. C. Theory and Modeling of Ion−Molecule Radiative Association Kinetics. *J. Chem. Phys.* **1996**, *104*, 4502−4516.
(104) Khare, B. N.; Bakes, E. L. O.; Imanaka, H.; McKay, C. P.; Cruikshank, D. P.; Arakawa, E. T. Analysis of the Time-Dependent Chemical Evolution of Titan Haze Tholin. *Icarus* **2002**, *160*, 172−182.
(105) Flasar, F. M.; Achterberg, R. K. The Structure and Dynamics of Titan's Middle Atmosphere. *Philos. Trans. R. Soc., A* **2009**, *367*, 649−664.
(106) Kislov, V. V.; Sadovnikov, A. I.; Mebel, A. M. Formation Mechanism of Polycyclic Aromatic Hydrocarbons beyond the Second Aromatic Ring. *J. Phys. Chem. A* **2013**, *117*, 4794−4816.
(107) Parker, D. S. N.; Kaiser, R. I.; Kostko, O.; Troy, T. P.; Ahmed, M. Unexpected Chemistry from the Reaction of Naphthyl plus Acetylene Molecules. *Angew. Chem., Int. Ed.* **2015**, *54*, 5421−5424.
(108) Parker, D. S. N.; Yang, T.; Dangi, B. B.; Kaiser, R. I.; Bera, P.; Lee, T. J. Low Temperature Formation of Nitrogen-Substituted Polycyclic Aromatic Hydrocarbons (NPAHs) - Barrierless Routes to Dihydro(iso)quinolines. *Astrophys. J.* **2015**, *815*, 115.
(109) Parker, D. S. N.; Kaiser, R. I.; Kostko, O.; Troy, T. P.; Ahmed, M.; Mebel, A. M.; Tielens, A. G. G. M. On the Synthesis of (Iso)Quinoline in Circumstellar Envelopes and Its Role in the Formation of Nucleobases in the Interstellar Medium. *Astrophys. J.* **2015**, *803*, 53.
(110) Landera, A.; Mebel, A. M. Low-Temperature Mechanisms for the Formation of Substituted Azanaphthalenes through Consecutive CN and C_2H Additions to Styrene and N-Methylenebenzenamine: A Theoretical Study. *J. Am. Chem. Soc.* **2013**, *135*, 7251−7263.

DOI: 10.1021/acs.jpca.6b09735
J. Phys. Chem. A 2017, 121, 901−926